factors. *Cell* **126**, 663–676.
Tang F, Kaneda M, OCarroll D *et al.* 2007 Maternal microRNAs are essential for mouse zygotic development. *Genes and Development* **21**, 644–648.
Tsuji-Takayama K, Inoue T, Ijiri Y *et al.* 2004 Demethylating agent, 5-azacytidine, reverses differentiation of embryonic stem cells. *Biochemical and Biophysical Research Communications* **323**, 86–90.
Vaziri H, West MD, Allsopp RC *et al.* 1997 ATM-dependent telomere loss in aging human diploid fibroblasts and DNA damage lead to the post-translational activation of p53 protein involving poly(ADP-ribose) polymerase. *EMBO Journal* **16**, 18–33.
Verlinsky Y, Strelchenko N, Kukharenko V *et al.* 2005 Human embryonic stem cell lines with genetic disorders. *Reproductive BioMedicine Online* **10**, 105–110.
Wakayama T, Tabar V, Rodriguez I *et al.* 2001 Differentiation of embryonic stem cell lines generated from adult somatic cells by nuclear transfer. *Science* **292**, 740–743.
Wakayama T, Tateno H, Mombaerts P, Yanagimachi R 2000 Nuclear transfer into mouse zygotes. *Nature Genetics* **24**, 108–109.
Wakayama T, Perry AC, Zuccotti M *et al.* 1998 Full-term development of mice from enucleated oocytes injected with cumulus cell nuclei. *Nature* **394**, 369–374.
Weismann A 1893 The Germ-Plasm: A Theory of Heredity. Charles Scribner's Sons, New York.
Weiss MC, Chaplain M 1971 Expression of differentiated functions in hepatoma cell hybrids: reappearance of tyrosine aminotransferase inducibility after the loss of chromosomes. *Proceedings of the National Academy of Sciences of the USA* **68**, 3026–3030.
Wernig M, Meissner A, Foreman R *et al.* 2007 In vitro reprogramming of fibroblasts into a pluripotent ES-cell-like state. *Nature* **448**, 318–324.
Willadsen SM 1986 Nuclear transplantation in sheep embryos. *Nature* **320**, 63–65.
Wilmut I, Schnieke AE, McWhir J *et al.* 1997 Viable offspring derived from fetal and adult mammalian cells. *Nature* **385**, 810–813.
Wobus AM, Boheler KR 2005 Embryonic stem cells: prospects for developmental biology and cell therapy. *Physiological Reviews* **85**, 635–678.
Wright WE, Brasiskyte D, Piatyszek MA, Shay JW 1996 Experimental elongation of telomeres extends the lifespan of immortal x normal cell hybrids. *EMBO Journal* **15**, 1734–1741.
Yamanaka S 2007 Strategies and new developments in the generation of patient-specific pluripotent stem cells. *Cell Stem Cell* **1**, 39–44.
Yamazaki Y, Fujita TC, Low EW *et al.* 2006 Gradual DNA demethylation of the Oct4 promoter in cloned mouse embryos. *Molecular Reproduction and Development* **73**, 180–188.
Yekta S, Shih IH, Bartel DP. 2004 MicroRNA-directed cleavage of HOXB8 mRNA. *Science* **304**, 594–596.

Received 27 July 2007; refereed 12 September 2007; accepted 17 October 2007.

Possible Involvement of CD81 in Acrosome Reaction of Sperm in Mice

MAYA TANIGAWA,[1,2] KIYOKO MIYAMOTO,[1] SATOSHI KOBAYASHI,[3] MASAHIRO SATO,[4] HIDENORI AKUTSU,[1] MASARU OKABE,[2,5] EISUKE MEKADA,[3] KEIICHI SAKAKIBARA,[1] MAMI MIYADO,[1] AKIHIRO UMEZAWA,[1] AND KENJI MIYADO[1,6,7]*

[1]*Department of Reproductive Biology and Pathology, National Center for Child Health and Development, Tokyo, Japan*
[2]*Faculty of Pharmaceutical Sciences, Osaka University, Osaka, Japan*
[3]*Research Institute for Microbial Diseases, Osaka University, Osaka, Japan*
[4]*Frontier Science Research Center, Kagoshima University, Kagoshima, Japan*
[5]*Genome Information Research Center, Osaka University, Osaka, Japan*
[6]*PREST, Japan Science and Technology Agency, Saitama, Japan*
[7]*School of Biomedical Science, Tokyo Medical and Dental University, Tokyo, Japan*

ABSTRACT Tetraspanin CD81 is closely homologous in amino acid sequence with CD9. CD9 is well known to be involved in sperm–egg fusion, and CD81 has also been reported to be involved in membrane fusion events. However, the function of CD81 as well as that of CD9 in membrane fusion remains unclear. Here, we report that disruption of the mouse CD81 gene led to a reduction in the fecundity of female mice, and CD81−/− eggs had impaired ability to fuse with sperm. Furthermore, we demonstrated that when CD81−/− eggs were incubated with sperm, some of the sperm that penetrated into the perivitelline space of CD81−/− eggs had not yet undergone the acrosome reaction, indicating that the impaired fusibility of CD81−/− eggs may be in part caused by failure of the acrosome reaction of sperm. In addition, we showed that CD81 was highly expressed in granulosa cells, somatic cells that surround oocytes. Our observations suggest that there is an interaction between sperm and CD81 on somatic cells surrounding eggs before the direct interaction of sperm and eggs. Our results may provide new clues for clarifying the cellular mechanism of the acrosome reaction, which is required for sperm–egg fusion. *Mol. Reprod. Dev.* © 2007 Wiley-Liss, Inc.

Key Words: CD9; acrosome reaction; fertilization; mice; zona pellucida

INTRODUCTION

Fertilization is accomplished by the direct interaction of sperm and eggs, a process mediated primarily by predicted, but yet unidentified gamete membrane proteins. In fertilization, the acrosome reaction is a change in sperm that is required for penetration into the zona pellucida, the egg coat, and facilitates the subsequent fusion with the egg plasma membrane (Moreno and Alvarado, 2006). Zona pellucida protein 3 (ZP3), one of the components forming the meshwork of the zona pellucida, has been considered to be the prime physiological inducer of the acrosome reaction in sperm, although the frequency of acrosome reaction is low after incubation with recombinant ZP3 (Beebe et al., 1992). This discrepancy suggests that, besides ZP3, unknown major factor(s) might be responsible for the acrosome reaction. To date, despite the importance of the acrosome reaction in fertilization, the underlying cellular mechanisms that regulate the acrosome reaction remain unclear.

Two tetraspanins, CD9 and CD81, are known to be important in the membrane fusion events in various biological systems. In virus-host cell fusion, human CD81 has been identified as a co-receptor for hepatitis C virus (Higginbottom et al., 2000; Cormier et al., 2004). Both CD9 and CD81 have been implicated in myoblast fusion (Tachibana and Hemler, 1999; Schwander et al., 2003) and monocyte/macrophage fusion in mice (Takeda et al., 2003). Recent studies using gene-targeting techniques demonstrated that female mice carrying a deletion of the CD9 gene produce eggs that mature normally but are defective in sperm–egg fusion (Kaji et al., 2000; Le Naour et al., 2000; Miyado et al., 2000; Takahashi et al., 2001). CD81 has also been reported to be expressed on the plasma membrane of unfertilized mouse eggs (Takahashi et al., 2001). Furthermore, CD81−/− mice have been reported to have defects in reproduction after several generations of backcrossing (Deng et al., 2000).

Grant sponsor: Precursory Research for Embryonic Science and Technology (PRESTO); Grant sponsor: The Ministry of Health, Labour and Welfare; Grant sponsor: The Ministry of Education, Culture, Sports, and Technology, of Japan.

*Correspondence to: Kenji Miyado, National Center for Child Health and Development, 2-10-1 Okura, Setagaya, Tokyo 157-8535, Japan. E-mail: kmiyado@nch.go.jp

Received 31 October 2006; Accepted 8 December 2006
Published online in Wiley InterScience (www.interscience.wiley.com).
DOI 10.1002/mrd.20709

Recently, Rubinstein et al. (2006) provided more detailed data showing that eggs of CD81−/− mice are unable to be fertilized with sperm, although the degree of the defect appeared not to be severe compared with that of CD9−/− eggs. Moreover, injection of CD9−/− eggs with mouse CD81 mRNA revealed that mouse CD81 was only moderately effective at reversing the infertility of CD9−/− eggs (Kaji et al., 2002). These findings taken together indicate that CD81 and CD9 each have different roles in fertilization.

Here we studied the role of CD81 in fertilization by in vitro fertilization (IVF) and immunohistochemical analysis, and propose a possible role of CD81 in the acrosome reaction in sperm.

MATERIALS AND METHODS

Animals

CD81−/− mice (Miyazaki et al., 1997) were kindly provided by Dr. Miyazaki and were backcrossed to C57BL/6 mice. Genotyping was carried out using polymerase chain reaction as previously described (Miyazaki et al., 1997). To visualize acrosome-intact sperm, EGFP-transgenic mice expressing EGFP in the acrosomes were generated by pronuclear injection of constructs carrying the EGFP gene driven by the mouse acrosin promoter (Nakanishi et al., 1999) and the DsRed2 gene tagged with a mitochondrial transport signal and driven by the CAG promoter into fertilized eggs of BDF1 mice (unpublished information). After the sperm were acrosome-reacted, EGFP was lost from the sperm heads and DsRed remained in the mitochondria of the mid-piece region. All animal procedures were performed according to protocols approved by the National Center for Child Health and Development and use committees.

Egg Collection

Female mice (aged 8–15 weeks) were injected with 5 U of hCG (Gonatropin; Aska Pharmaceutical Co., Ltd, Tokyo, Japan) 48 hr after administration of 5 U of PMSG (Serotropin; Aska Pharmaceutical Co., Ltd). Ovulated eggs were collected from the oviductal ampulla 13.5–15 hr after hCG injection, and placed in 100-μl drops of TYH medium equilibrated with 5% CO_2 in air at 37°C. Cumulus cells were removed with 300 IU/ml of hyaluronidase (H-3506, Sigma-Aldrich, Missouri, MO), and eggs were incubated with a defined number of sperm.

Sperm Preparation and In Vitro Fertilization

Sperm were collected by squeezing two cauda epididymides of 8- to 10-week-old B6C3F1 or transgenic male mice in a well containing 100-μl of TYH medium. Sperm were incubated at 37°C in 5% CO_2 for 90 min before being mixed with eggs derived from wild-type or CD81−/− female mice. The final concentration of sperm added to an egg-containing drop was 1.5×10^5 sperm/ml. To examine the rate of fertilization, we counted the number of eggs at the two-cell stage 24 hr after incubation with the sperm. For counting the number of fused sperm, the zona pellucida was removed from the eggs by a brief incubation in acid Tyrode solution, and sperm were incubated with eggs preloaded with 4′,6-diamidino-2-phenylindole (DAPI) for counting the number of sperm fused with eggs (Yamagata et al., 2002). For counting the number of acrosome-intact sperm, EGFP-expressing sperm were incubated with zona-intact CD81+/+ or CD81−/− eggs. The eggs were all subjected to confocal microscopic analysis for the presence of sperm exhibiting red and green fluorescence or red fluorescence alone within the perivitelline space 4 hr after incubation.

Immunostaining

For immunostaining of cryostat sections, ovaries from 8- to 10-week-old wild-type C57BL/6 females were fixed in 2% paraformaldehyde in PBS (−) for 2 days at 4°C, and then immersed in 30% sucrose in PBS (−) for more than 2 days at 4°C, embedded in Tissue-Tek OCT compound (Sakura Finetek Co., Tokyo, Japan), and finally frozen before serial cryostat sectioning (8 μm in thickness). Slides were fixed in an acetone and incubated with anti-CD81 antibody (Eat-1) diluted 1:300 in PBS (−) containing 0.1% bovine serum albumin (BSA), BSA/PBS (−), or anti-ZP3 antibody diluted 1:300 in BSA/PBS (−), overnight at 4°C. After washing three times with BSA/PBS (−), the samples were incubated with Alexa 546-conjugated goat anti-hamster IgG (A-21111, Invitrogen, California, CA) or Alexa 488-conjugated goat anti-rat IgG (A-11006, Invitrogen) for 2 hr at room temperature. After extensive washing, the slides were inspected for fluorescence using LSM 510 META confocal microscope.

Immunoblotting

Samples containing equal amounts of eggs were dissolved in nonreducing sample buffer and subjected to 12% SDS–PAGE according to procedures described previously (Miyado et al., 2000). After electrophoresis, the gels were transferred to PVDF membranes for immunoblot analysis. The blots were blocked in 1% nonfat dry milk, and were probed with the primary antibodies, anti-mouse CD81 antibody (Eat-1, BD Biosciences, California, CA) or anti-mouse CD9 antibody (KMC8, BD Biosciences). After washing in TBS-Tween buffer, the membranes were incubated with HRP-labeled secondary antibodies; goat anti-rat antibody or goat anti-hamster antibody. The expression level of immunoreacted products was determined by treatment of the blots with an ECL or ECL Plus Detection Kit (GE Healthcare Bio-Science Co., New Jersey, UK) and exposure to X-ray film at room temperature.

Statistical Analysis

Data from different groups were tested by the *t*-test for the significance of the difference between the means of two independent samples using the computer software KaleidaGraph (version 3.6, Synergy Software, Inc., Pennsylvania, PA).

RESULTS

Female Fertility Impaired by CD81 Deficiency

Figure 1A depicts the average litter size in matings of three genotypes of females, wild-type, CD81+/− and CD81−/− mice, with CD81+/− males over a period of 6 months. Although these females displayed normal mating behavior with the males (data not shown), the average litter size of CD81−/− females was markedly reduced relative to those of CD81+/− and wild-type mice (on average, 1.3 ± 2.5 vs. 11.3 ± 1.3 and 11.0 ± 0.8) (Fig. 1A). To examine the oocyte maturation and ovulation, we also collected the eggs from mice superovulated by stimulation with exogenous gonadotropin. The eggs collected from CD81−/− mice were indistinguishable with regard to morphology and number (on average, 18.0 ± 2.8) from those wild-type and CD81+/− mice (on average, 19.9 ± 1.7 and 21.7 ± 2.8) (Fig. 1B). Therefore, the reduction in fertility of CD81−/− females did not seem to be due to defects of ovulation or oocyte maturation.

Involvement of CD81 in Fertilization

To clarify the cause of the reduced fertility of CD81−/− females, the function of CD81−/− eggs was further examined by IVF. When cumulus oocyte complexes (COCs) collected from CD81−/− or wild-type control mice were incubated with the wild-type sperm, the sperm could disperse cumulus cells, somatic cells surrounding eggs, and reach and apparently penetrate the zona pellucida of CD81−/− and wild-type eggs. However, the average rate of eggs developing to the two-cell stage was substantially decreased for CD81−/− eggs (on average, $15.0 \pm 2.5\%$) compared with that for wild-type eggs (on average, $65.0 \pm 10.8\%$) 24 hr after incubation with the sperm (Fig. 1D). Furthermore, in CD81−/− eggs, several sperm were observed in the perivitelline space (Fig. 1C). The delayed formation of two-cell embryos and the accumulation of more than one sperm within the perivitelline space in CD81−/− eggs demonstrate that CD81−/− eggs have impaired ability of fertilization. Subsequently, to examine the cause of the impaired fertilization, we performed IVF for CD81−/− eggs and wild-type eggs after the zona pellucida was removed using acid Tyrode solution (Fig. 2A,B). To measure the number of sperm fused with eggs, both types of eggs were preloaded with DAPI before incubation with wild-type sperm (Yamagata et al., 2002). One hour after insemination, estimation of the average number of sperm fused with one egg by measurement of DAPI fluorescence revealed that CD81−/− eggs showed a decreased number of fused sperm (on average, 1.21 ± 0.23) in comparison with the wild-type eggs (on average, 1.95 ± 0.27). Those results suggest that CD81 is involved in sperm–egg fusion, either directly or indirectly.

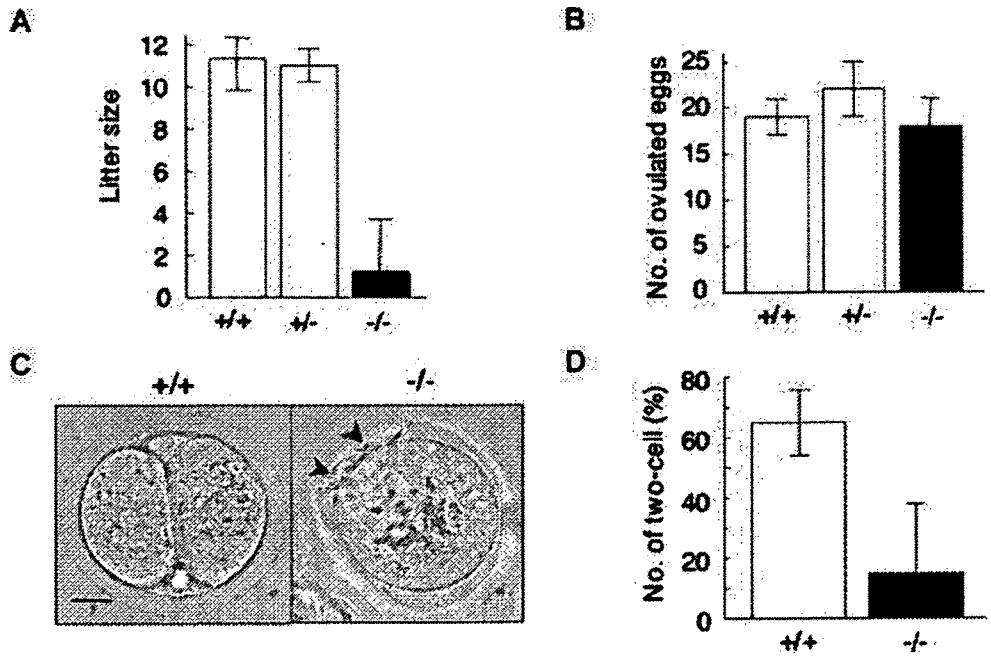

Fig. 1. Female infertility caused by CD81 deficiency. **A**: Average litter sizes of crosses between CD81+/− males and three types of females, wild-type, CD81+/− and CD81−/− mice. Each of the mating pairs was kept in a separate cage, and births over a 6-month period were monitored. Data of births during successive 2-month periods were grouped together, and the average litter size of wild-type, CD81+/− and CD81−/− females was calculated from data recorded for five mating pairs 8–15 weeks of age at the start of the experiment. **B**: Average number of ovulated eggs from wild-type, CD81+/− and CD81−/− female mice. The eggs were collected 13.5–16 hr after hCG treatment, and counted. **C**: Representative micrographs of CD81+/+ and CD81−/− eggs. The eggs were obtained 24 hr after incubation with the wild-type sperm. **D**: Average number of eggs that developed to the two-cell stage 24 hr after incubation with the wild-type sperm. The black bars show the results for CD81−/− eggs (A,B,D). Error bars represent SEM (A,B,D). Scale bar, 20 μm (C).

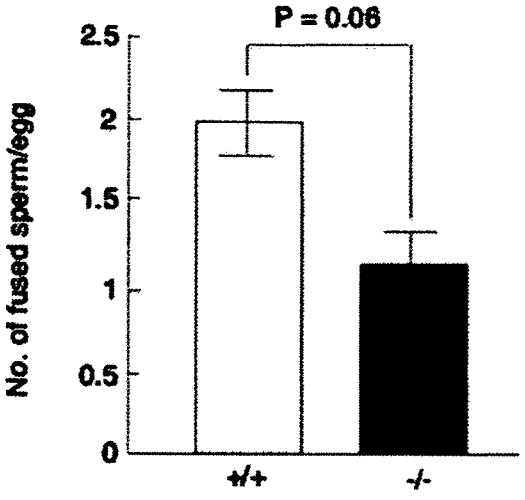

Fig. 2. In vitro sperm–egg fusion. Average number of sperm fused with wild-type or CD81−/− eggs after 3 hr of incubation. Error bars represent SEM. Data from different groups were tested by the *t*-test for the significance of the difference between the means of two independent samples ($P = 0.06$).

Expression of CD9 in CD81−/− Eggs

The mechanisms by which CD81 acts are still unclear. However, CD81 tends to form multimolecular complexes in which tetraspanins associate with specific proteins depending on the type of cell. In B cells, CD81 directly associates with CD19, taking part in the CD19-CD21-CD81 signaling complex (Pileri et al., 1998), which accords with the evidence that the expression of CD19 in bone marrow, spleen, and peripheral B cells is reduced in CD81−/− mice (Miyazaki et al., 1997). As previously mentioned, CD9 on the egg plasma membrane is required for fusion with sperm, and the impaired fusibility of CD81−/− eggs with sperm may likely be dependent on the expression of CD9. To investigate whether CD81 deficiency may cause downregulation of CD9 expression, the expression level of CD9 was examined (Fig. 3). We collected three types of eggs, wild-type, CD81+/− and CD81−/− eggs, 13.5–15 hr after hCG injection into mice, and examined the expression level of CD9 in comparison with that of CD81 by SDS–PAGE. The amounts of CD81 were invariable in wild-type and CD81+/− eggs, but CD81 was lost in CD81−/− eggs. By contrast, there were no significant differences in the expression of CD9 among these eggs. Therefore, the impairment of fertilization caused by CD81 deficiency cannot be attributed to decreased expression of CD9 in eggs.

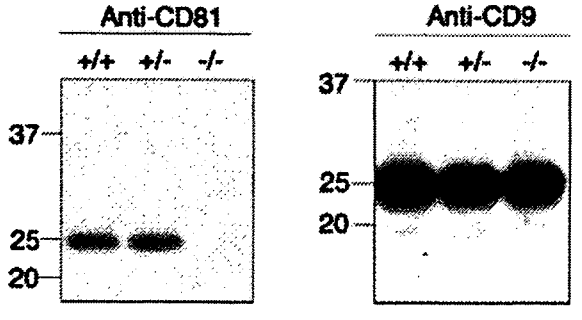

Fig. 3. The expression of CD9 in wild-type, CD81+/− and CD81−/− eggs. Proteins were isolated from the types of eggs indicated and resolved by sodium dodecyl sulfate polyacrylamide gel electrophoresis under nonreducing conditions. The proteins were electrophoretically transferred to a membrane, where they were probed with antibodies to CD81 (**panel A**) and CD9 (**panel B**). The proteins corresponding to each 110 egg (panel A) and 10 eggs (panel B) were analyzed.

Expression of CD81 During Folliculogenesis

The expression and localization of CD81 in ovarian tissues were immunohistochemically assessed using cryostat sections of adult wild-type ovaries. The follicles consist of immature eggs and granulosa cells that surround the egg; a single follicle usually grows to the preovulatory stage and releases the egg for potential fertilization (Buccione et al., 1990). Immunohistochemical staining with anti-CD81 mAb demonstrated that CD81 was continuously expressed in the egg and surrounding follicles (Fig. 4), and in cumulus cells surrounding ovulated eggs (data not shown). These data indicate that the sperm may encounter CD81 on the somatic cells surrounding eggs before direct interaction of sperm and eggs.

Possible Involvement of CD81 in Acrosome Reaction

Based on the localization of CD81 and the impaired fertilization of CD81−/− eggs, we speculated that the inability of wild-type sperm to fuse CD81−/− eggs might be due to impairment of prefusional stages, including the acrosome reaction. To examine the involvement of CD81 in the acrosome reaction of the sperm, CD81−/− eggs or wild-type eggs were incubated with the sperm collected from transgenic mice specifically expressing enhanced green fluorescent protein (EGFP) in the acrosomes (Fig. 5). The acrosome corresponds functionally to a lysosome and thus contains lysosomal enzymes (Moreno and Alvarado, 2006), and acrosin is a sperm acrosomal serine proteinase that is lost from the sperm head after the acrosome reaction is completed (Baba et al., 1994). Therefore, sperm expressing EGFP at the acrosomes in the heads are useful for the detection of acrosome-intact sperm. After 3 hr of incubation, we counted the number of acrosome-intact sperm within the perivitelline spaces. To count the sperm that had penetrated into the zona pellucida, the eggs were incubated with 3.0×10^5 sperm/ml. When the number of sperm within the perivitelline space were counted 3 hr after incubation with the eggs, we observed that an increased percentage ($8.5 \pm 2.3\%$) of the sperm that had penetrated into the perivitelline space of CD81−/− eggs exhibited EGFP fluorescence in their head portion. In contrast, very few sperm that had penetrated into the perivitelline space of wild-type eggs exhibited green fluorescence ($1.4 \pm 1.0\%$). These results suggest that the sperm that penetrated into the zona pellucida of the CD81−/− eggs were impaired in the acrosome reaction.

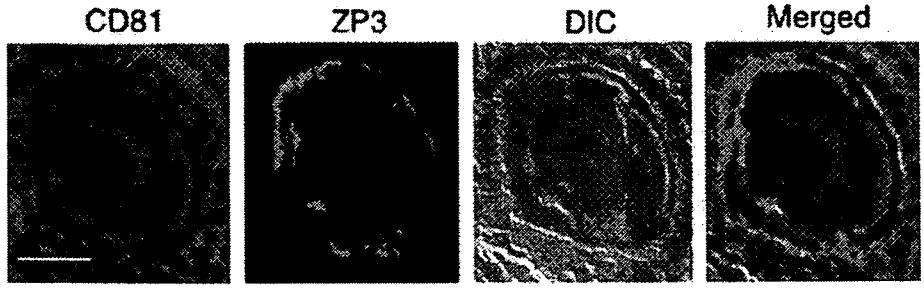

Fig. 4. CD81 is expressed at high levels in granulosa cells during oogenesis. Frozen sections of ovaries from wild-type mice were stained with anti-mouse CD81 mAb and with anti-ZP3 mAb. DIC represents a photograph taken by differential interference contrast. Scale bar, 20 μm. [See color version online at www.interscience.wiley.com.]

DISCUSSION

CD81 has been suggested to be a protein playing a role in membrane fusion events, but the function of CD81 in sperm–egg fusion remains unknown. As suggested by Rubinstein et al. (2006), CD9 and CD81 may have different roles in sperm–egg fusion. This notion is supported by the following facts: (1) deletion of a single gene, CD9 or CD81, causes impaired fertilization, and the expression of CD9 on eggs is not perturbed by CD81 deficiency, and (2) CD9−/− eggs injected with mRNA encoding CD81 cannot be fully rescued to the same degree as those injected with CD9 mRNA (Kaji et al., 2002).

Generally, the acrosome reaction is a change in the membrane of sperm that are activated for penetration into zona pellucida and facilitates the subsequent fusion with the egg membrane (Baba et al., 1994). During the acrosome reaction, the disruption of the acrosome covering the sperm head causes the release of acrosin and other proteolytic substances. As previously reported (Moreno and Alvarado, 2006), these materials included in the acrosome are important for the penetration of sperm into the zona pellucida and for sperm–egg fusion, but the molecular mechanism underlying the acrosome reaction is largely unknown. When wild-type eggs were incubated with sperm expressing EGFP in the acrosomes, we found the presence of acrosome-intact

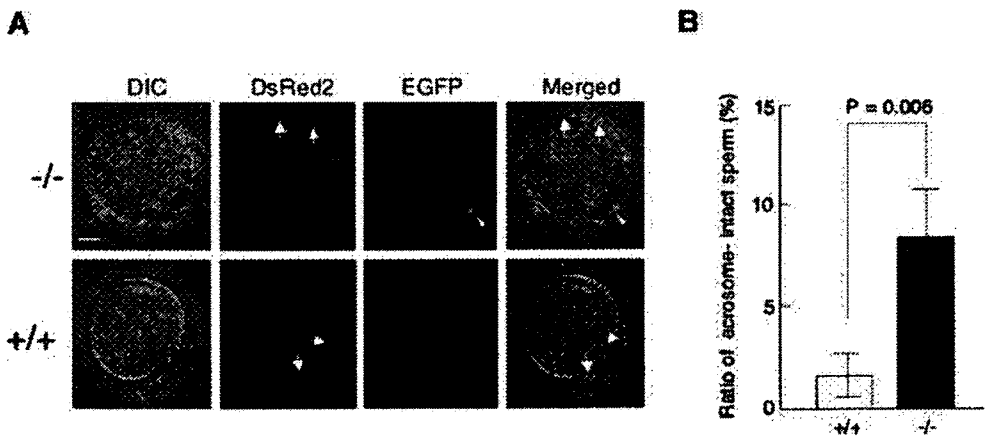

Fig. 5. In vitro fertilization assay for acrosome reaction. **A**: Representative photographs. CD81−/− eggs were incubated with transgenic sperm expressing EGFP at acrosomes in the sperm heads. Eggs from wild-type females were also subjected to fertilization using the AR-GFP transgenic sperm as controls. Four hours after insemination, the eggs were inspected for fluorescence using a confocal microscope. As shown in the **upper panel**, some CD81−/− eggs had sperm with green fluorescence (indicated by arrowheads) in their head region in the perivitelline space, while almost no wild-type eggs had such types of sperm (**lower panel**). Photomicrographs taken under light (DIC); photomicrographs taken for detecting DsRed2 translocated to mitochondria by the retention signal (Mt-DsRed2) and specifically expressed in the mid-piece of sperm (indicated by arrows); photomicrographs taken for detecting EGFP-derived green fluorescence specifically expressed in the head region of sperm (indicated by arrowheads); merged images. Scale bar, 20 μm. **B**: Examination of acrosome reaction using EGFP-expressing sperm. CD81−/− or wild-type eggs were fertilized in vitro with epididymal sperm expressing EGFP in the acrosomes. Four hours after insemination, the sperm entering into the perivitelline space were inspected for fluorescence using a confocal microscope. Note that the number of sperm carrying intact acrosomes (exhibiting green fluorescence in the sperm head region, as shown in A) and entering into the perivitelline space of CD81−/− eggs was significantly higher than that of acrosome-intact sperm entering into the perivitelline space of wild-type eggs. Acrosome-intact sperm can easily be detected since they exhibit bright green fluorescence in their head region. The total number of sperm entered into perivitelline space can be counted by inspection for red fluorescence in the mid-piece of the sperm. [See color version online at www.interscience.wiley.com.]

sperm in the outer layer of the zona pellucida (data not shown), but almost all sperm that penetrated into the perivitelline space had lost the acrosome caps (Fig. 5). These findings suggest that the acrosome reaction may occur in the perivitelline space and/or inner layer of the zona pellucida.

Another possible reason for the failure of the acrosome reaction of EGFP-expressing sperm in CD81−/− eggs is that "zona hardening" in CD81−/− eggs may not be sufficient compared to that in wild-type eggs. The weakened zona hardening might permit the penetration of some acrosome-intact sperm into CD81−/− eggs. However, since proteins other than components forming the zona pellucida may be triggers for preventing polyspermy and zona hardening (Sun, 2003), it would be of interest to test whether CD81 and ZP3 interact with each other.

In conclusion, the results of our IVF experiments suggest the possible involvement of CD81 in the acrosome reaction of zona pellucida-penetrated sperm prior to the fusion of sperm with eggs. Extensive attempts to elucidate the role of CD81 in the acrosome reaction are now underway.

ACKNOWLEDGMENTS

We are thankful for Dr. Tsujimoto (Faculty of Medicine, Osaka University) for kindly providing mt-DsRed2 contract for transgenic production. This work was supported by a grant from Precursory Research for Embryonic Science and Technology (PRESTO), The Ministry of Health, Labour and Welfare, and a grant-in aid for Scientific Research, The Ministry of Education, Culture, Sports, and Technology, of Japan.

REFERENCES

Baba T, Azuma S, Kashiwabara S, Toyoda Y. 1994. Sperm from mice carrying a targeted mutation of the acrosin gene can penetrate the oocyte zona pellucida and effect fertilization. J Biol Chem 269: 31845–31849.

Beebe SJ, Leyton L, Burks D, Ishikawa M, Fuerst T, Dean J, Saling P. 1992. Recombinant mouse ZP3 inhibits sperm binding and induces the acrosome reaction. Dev Biol 151:48–54.

Buccione R, Schroeder AC, Eppig JJ. 1990. Interactions between somatic cells and germ cells throughout mammalian oogenesis. Biol Reprod 43:543–547.

Cormier EG, Tsamis F, Kajumo F, Durso RJ, Gardner JP, Dragic T. 2004. CD81 is an entry coreceptor for hepatitis C virus. Proc Natl Acad Sci USA 101:7270–7274.

Deng J, Yeung VP, Tsitoura D, DeKruyff RH, Umetsu DT, Levy S. 2000. Allergen-induced airway hyperreactivity is diminished in CD81-deficient mice. J Immunol 165:5054–5061.

Higginbottom A, Quinn ER, Kuo CC, Flint M, Wilson LH, Bianchi E, Nicosia A, Monk PN, McKeating JA, Levy S. 2000. Identification of amino acid residues in CD81 critical for interaction with hepatitis C virus envelope glycoprotein E2. J Virol 74:3642–3649.

Kaji K, Oda S, Miyazaki S, Kudo A. 2002. Infertility of CD9-deficient mouse eggs is reversed by mouse CD9, human CD9, or mouse CD81; polyadenylated mRNA injection developed for molecular analysis of sperm-egg fusion. Dev Biol 247:327–334.

Kaji K, Oda S, Shikano T, Ohnuki T, Uematsu Y, Sakagami J, Tada N, Miyazaki S, Kudo A. 2000. The gamete fusion process is defective in eggs of Cd9-deficient mice. Nat Genet 24:279–282.

Le Naour F, Rubinstein E, Jasmin C, Prenant M, Boucheix C. 2000. Severely reduced female fertility in CD9-deficient mice. Science 287:319–321.

Miyado K, Yamada G, Yamada S, Hasuwa H, Nakamura Y, Ryu F, Suzuki K, Kosai K, Inoue K, Ogura A, Okabe M, Mekada E. 2000. Requirement of CD9 on the egg plasma membrane for fertilization. Science 287:321–324.

Miyazaki T, Muller U, Campbell KS. 1997. Normal development but differentially altered proliferative responses of lymphocytes in mice lacking CD81. EMBO J 16:4217–4225.

Moreno RD, Alvarado CP. 2006. The mammalian acrosome as a secretory lysosome: New and old evidence. Mol Reprod Dev 73:1430–1434.

Nakanishi T, Ikawa M, Yamada S, Parvinen M, Baba T, Nishimune Y, Okabe M. 1999. Real-time observation of acrosomal dispersal from mouse sperm using GFP as a marker protein. FEBS Lett 449:277–283.

Pileri P, Uematsu Y, Campagnoli S, Galli G, Falugi F, Petracca R, Weiner AJ, Houghton M, Rosa D, Grandi G, Abrignani S. 1998. Binding of hepatitis C virus to CD81. Science 282:938–941.

Rubinstein E, Ziyyat A, Prenant M, Wrobel E, Wolf JP, Levy S, Le Naour F, Boucheix C. 2006. Reduced fertility of female mice lacking CD81. Dev Biol 290:351–358.

Schwander M, Leu M, Stumm M, Dorchies OM, Ruegg UT, Schittny J, Muller U. 2003. Beta1 integrins regulate myoblast fusion and sarcomere assembly. Dev Cell 4:673–685.

Sun QY. 2003. Cellular and molecular mechanisms leading to cortical reaction and polyspermy block in mammalian eggs. Microsc Res Tech 61:342–348.

Tachibana I, Hemler ME. 1999. Role of transmembrane 4 superfamily (TM4SF) proteins CD9 and CD81 in muscle cell fusion and myotube maintenance. J Cell Biol 146:893–904.

Takahashi Y, Bigler D, Ito Y, White JM. 2001. Sequence-specific interaction between the disintegrin domain of mouse ADAM 3 and murine eggs: Role of beta1 integrin-associated proteins CD9, CD81, and CD98. Mol Biol Cell 12:809–820.

Takeda Y, Tachibana I, Miyado K, Kobayashi M, Miyazaki T, Funakoshi T, Kimura H, Yamane H, Saito Y, Goto H, Yoneda T, Yoshida M, Kumagai T, Osaki T, Hayashi S, Kawase I, Mekada E. 2003. Tetraspanins CD9 and CD81 function to prevent the fusion of mononuclear phagocytes. J Cell Biol 161:945–956.

Yamagata K, Nakanishi T, Ikawa M, Yamaguchi R, Moss SB, Okabe M. 2002. Sperm from the calmegin-deficient mouse have normal abilities for binding and fusion to the egg plasma membrane. Dev Biol 250:348–357.

Available online at www.sciencedirect.com
ScienceDirect
Biochemical and Biophysical Research Communications 364 (2007) 838–843
BBRC
www.elsevier.com/locate/ybbrc

Preferential localization of SSEA-4 in interfaces between blastomeres of mouse preimplantaion embryos

Ban Sato [a,e], Yohko U. Katagiri [a,d,*], Kenji Miyado [b], Hidenori Akutsu [b], Yoshitaka Miyagawa [a], Yasuomi Horiuchi [a], Hideki Nakajima [a], Hajime Okita [a,d], Akihiro Umezawa [b], Jun-ichi Hata [a], Junichiro Fujimoto [c,d,1], Kiyotaka Toshimori [e], Nobutaka Kiyokawa [a,d]

[a] *Department of Developmental Biology, National Research Institute for Child Health and Development, 2-10-1 Okura, Setagaya-ku, Tokyo 157-8535, Japan*
[b] *Department of Reproductive Biology, National Research Institute for Child Health and Development, 2-10-1 Okura, Setagaya-ku, Tokyo 157-8535, Japan*
[c] *National Research Institute for Child Health and Development, 2-10-1 Okura, Setagaya-ku, Tokyo 157-8535, Japan*
[d] *Core Research for Evolutional Science and Technology (CREST) of Japan Science and Technology Corporation (JST), Japan*
[e] *Department of Anatomy and Developmental Biology, Graduate School of Medicine, Chiba University, Chiba 260-8670, Japan*

Received 11 October 2007
Available online 26 October 2007

Abstract

The monoclonal antibody 6E2 raised against the embryonal carcinoma cell line NCR-G3 had been shown to also react with human germ cells. Thin-layer chromatography (TLC) immunostaining revealed that 6E2 specifically reacts with sialosylglobopentaosylceramide (sialylGb5), which carries an epitope of stage-specific embryonic antigen-4 (SSEA-4), known as an important cell surface marker of embryogenesis. The immunostaining of mouse preimplantation embryos without fixation showed that the binding of 6E2 caused the clustering and consequent accumulation of sialylGb5 at the interface between blastomeres. These results suggest that SSEA-4 actively moves on the cell surface and readily accumulates between blastomeres after binding of 6E2.

Keywords: SialylGb5; SSEA-4; Embryonic stem cells; Embryonal carcinoma cells; Preimplantation embryo; Immunostaining

Embryonal carcinoma (EC) cells isolated from teratocarcinomas have been shown to possess pluri- or multipotency in both mouse and human systems [1–3]. In mice, certain EC cells as well as embryonic stem (ES) cells have been considered to be developmentally equivalent to the inner cell mass of blastocysts [1]. These EC cells are useful for clarifying the molecular characteristics of early embryonic cells and thus many efforts have been made to establish EC cell lines and monoclonal antibodies (Mabs) that detect differentiation-related molecules on EC cells. As a consequence, a number of stage-specific markers for embryogenesis have been identified. Notably, it is important that this molecular information is adapted to research on ES cells or mouse preimplantation embryos. Stage-specific embryonic antigen (SSEA) -1, -3, and -4, as well as tumor rejection antigen (TRA) -1-60 and -1-81 [4], have been used as stage-specific markers for embryogenesis, though their functional significance in early development remains unclear. Interestingly, however, most of these antigens are carbohydrates themselves or closely related to the carbohydrates carried on glycosphingolipids (GSLs) and glycoproteins [5].

6E2 is a Mab established by immunizing with NCR-G3 cells, a previously established multipotent human EC cell

* Corresponding author. Address: Department of Developmental Biology, National Research Institute for Child Health and Development, 2-10-1 Okura, Setagaya-ku, Tokyo 157-8535, Japan. Fax: +81 3 3417 2496.
E-mail address: kata@nch.go.jp (Y.U. Katagiri).
[1] Vice General Director.

0006-291X/$ - see front matter © 2007 Elsevier Inc. All rights reserved.
doi:10.1016/j.bbrc.2007.10.093

line capable of differentiating into trophoblastic cell lineages other than somatic cells [3]. It has been revealed that 6E2 reacts with not only human ECs, including NCR-G2 and 3 cells, but also other germ cell tumors, as well as normal human germ cells such as spermatogonia and oocytes [6]. Although a previous study reported that 6E2 immunoprecipitates a cell surface protein having a molecular weight of approximately 80 kDa from ^{125}I-labeled NCR-G3 cells, the specific antigen recognized by 6E2 still remains unknown. To characterize the antigen specificity of 6E2, we examined the reactivity of the Mab with other cell lines using several distinct methods. In this paper, we present evidence that 6E2 recognizes SSEA-4 carried by sialylGb5. Using 6E2, we determined the localization of SSEA-4 in "living" mouse preimplantation embryos and observed its preferential localization in interface between blastomeres.

Materials and methods

Cells, antibodies, and animals. The human renal carcinoma cell line ACHN was purchased from American Type Culture Collection. The African green monkey kidney cell line Vero was a gift from Dr. T. Takeda of Department of Infectious Diseases Research, National Children's Medical Research Center, Tokyo, Japan. Cells were maintained in Dulbecco's modified Eagle's minimum essential medium (DMEM) (Sigma Chem., St. Louis, MO) supplemented with 10% fetal bovine serum (FBS) (JRH Bioscience, Lenexa, KS). The human EC cell line NCR-G2 [3] was cultured in a 1:1 mixture of DMEM and Ham's F12 medium (DMEM/F12) (Invitrogen Gibco, Carlsbad, CA) supplemented with 10% FBS(JRH Bioscience), non-essential amino acid solution (NEAA) (Invitrogen Gibco), and Insulin-Transferin-Sodium Selenite media (Invitrogen Gibco). The cynomolgus monkey ES cell line CMK-6 [7] were provided by Dr. Yasushi Kondo of Mitsubishi Tanabe Pharma Corporation. ES cells were grown on mouse embryonic fibroblast feeder cells that were inactivated by gamma-irradiation in DMEM/F12 supplemented with 20% Knockout™ Serum Replacement, 2 mM Glutamax-I, 1% NEAA, 50 units/ml penicillin, 50 μg/ml streptomycin, 0.1 mM 2-mercaptoethanol, 1% sodium pyruvate, and 5 ng/ml bFGF (all from Invitrogen GIBCO). The cultures were performed at 37 °C in a 5% CO_2 incubator. The human venous blood from a healthy consenting volunteer was drawn in a heparin-coated syringe. The blood was spun at 3000 rpm for 15 min and human red blood cells (hRBCs) were washed three times in phosphate buffered saline (PBS).

The conjugation of affinity-purified 6E2 (mouse IgG_3, κ) [6] to the fluorescence reagent was performed with an Alexa Fluor® 488 monoclonal antibody labeling kit (Molecular Probes, Eugene, OR.) according to the manufacturer's instructions. The anti-SSEA-4 Mabs used in this study were Raft.2 [8] and MC813-70 (R&D Systems, Inc Minneapolis, MN). Alexa Fluor® 488 goat anti-mouse IgG and Streptavidin Alexa Fluor® 568 were purchased from Molecular probes.

BDF_1 mice were purchased from Clea Japan (Tokyo, Japan).

TLC immunostaining of GSLs. TLC immunostaining of GSLs from cultured cells and hRBCs was performed as previously described [9]. Reference GSLs were purchased from Matlayer, Inc. (Pleasant Gap, PA). SialylGb5 was purified from ACHN cells by preparative TLC. Purified GM1 b was kindly provided by Dr. Nakamura of RIKEN, Saitama, Japan [10].

Flow cytometry. Cells were harvested and incubated with a primary antibody (1 μg/ml) for 1 h on ice, followed by treatment with fluorescein isothiocyanate-conjugated goat anti-mouse immunoglobulins (Jackson Immunoresearch Laboratories, Inc., West Grove, PA) at a dilution of 1:50 and analyzed with an EPICS-XL flow cytometer (Beckman Coulter, Inc, Miami, FL).

Dot blot analysis. Purified sialylGb5 was serially diluted (0.1–60 ng) and vacuum blotted onto a PVDF membrane by using a 96-well format dot blot apparatus (Bio-Rad Laboratories, Richmond, CA). The membrane was immunostained with the Mab 6E2 or MC813-70 (0.5 μg/ml) according to a previously described procedure [9]. The antibodies that bound to the membranes were visualized with ECL-plus Western Blotting Detection Reagents (GE Healthcare UK Ltd, Buckinghamshire, UK) and scanned with a LAS-1000 luminescent imaging analyzer (Fujifilm, Tokyo, Japan). Scanned images were analyzed using the software Image Gauge with which the LAS-1000 was equipped.

Indirect immunostaining of cynomolgus monkey ES cells. Cells were grown on a glass-bottomed dish (IWAKI) for 3 days and then these cells were fixed for 30 min with 4% paraformaldehyde in PBS and permeabilized with 0.2% Triton X-200 in PBS for 20 min. Subsequently, the cells were washed three times with PBS for 5 min and blocked with 5% normal goat serum in PBS for 30 min. The fixed cells were incubated with anti-SSEA-4 antibodies or isotype-matched mouse IgG at a dilution of 1:300 for 2 h, followed by incubation with Alexa Fluor® 488-conjugated goat anti-mouse IgG at a dilution of 1:300 for 30 min. DAPI was used for counter staining of nuclei.

Immunostaining of mouse preimplantation embryos. Mouse preimplantation embryos were collected from superovulated mice. Seven-week-old BDF1 female mice were induced to superovulate with intraperitoneal injections of pregnant mare's serum gonadotropin (ASKA Pharmaceutical co., Ltd., Tokyo, Japan) (5 IU) and human chorionic gonadotropin (hCG) (ASKA Pharmaceutical co) (5 IU) 48 h apart and mated with individual BDF1 male mice after the hCG injection. The 2-cell, the 8-cell, and the morula stage embryos were flushed out from oviducts at 36, 60, and 72 h after the hCG injection, respectively. Animals were treated according to the institutional animal care and use guidelines of National Research Institute for Child Health and Development.

Embryos immediately after being collected and those prefixed with 2% paraformaldehyde in Hepes buffered saline were incubated in 30 μl drops of M16 medium containing 0.45 μg of Alexa Fluor® 488-conjugated 6E2 for 1 h or biotinylated MC813-70 for 1 h, treated with streptavidin Alexa Fluor® 568 diluted 1:300, and then they were washed three times in 30 μl drops of M16 medium. All staining steps were carried out at 37 °C in a CO_2 incubator for fresh embryos and at 4 °C for fixed embryos. The stained embryos were placed in drop of a M16 medium on glass-bottomed dishes (IWAKI, Tokyo, Japan), and were observed with a LSM510 Zeiss Confocal laser-scanning microscope (Carl Zeiss, Thornwood, NY) to obtain a field of view of the embryo only with a 40× objective lens.

Results and discussion

6E2 specifically binds to sialylGb5

In order to examine whether the 80 kDa membrane protein is recognized by 6E2, we performed a Western analysis of the cell lysates or their immunoprecipitates with 6E2. Since no significant signal was detected on the blot (data not shown), we examined TLC immunostaining of GSLs extracted from several 6E2-positive cell lines. ACHN cells showed the expression of comparable amounts of Gb3, Gb4, Gb5, and sialylGb5, whereas Vero cells and NCR-G2 cells expressed predominantly Gb3 (Fig. 1A). TLC immunostaining analysis revealed that 6E2 binds to a major slow-migrating GSL extracted from these three cell lines. The slow-migrating GSL was identified as sialylGb5, defined by the Mab Raft.2. We observed that 6E2 bound to sialylGb5 (LKE-antigen) of hRBCs [13] (Fig. 1B). Finally, we examined the reactivity of 6E2 with purified GSLs and found that the Mab reacts with purified sialylGb5, but not purified GM1 b (Fig. 1C). These results indicate that 6E2 specifically binds to sialylGb5 and thus is an anti-SSEA-4

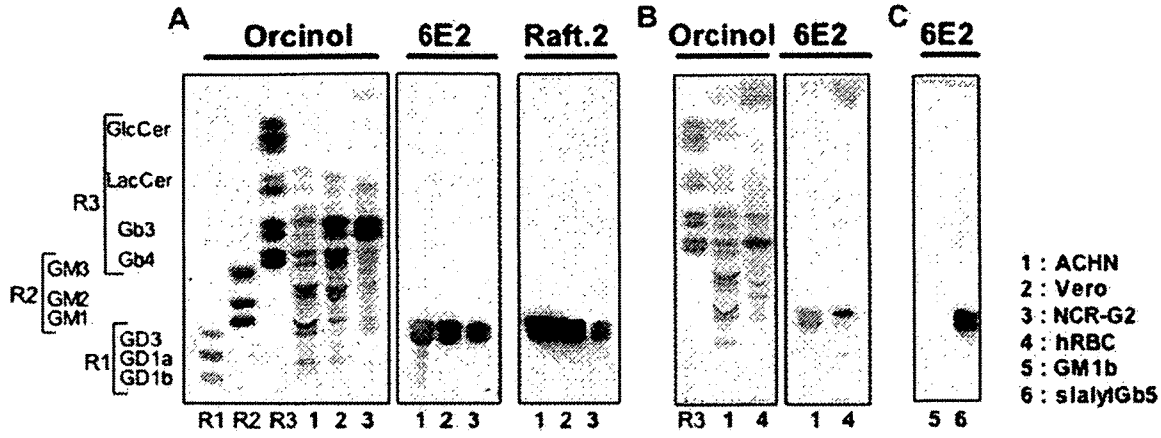

Fig. 1. TLC immunostaining of GSLs prepared from cultured cells and hRBCs. GSLs extracted from cultured cells and hRBCs or purified GSLs were separated by TLC in a solvent system of chloroform/methanol/water containing 0.2% $CaCl_2$ (5:4:1, v/v/v). Plates were chemically stained with orcinol-sulfurnic acid or were immunostained with 6E2 and Raft.2. Lane 1, ACHN; Lane 2, Vero; Lane 3, NCR-G2; Lane 4, hRBCs; Lane 5, GM1b; Lane 6, sialylGb5. Reference markers used were disialosyl gangliosides of GD3, GD1a, and GD1b (R1), monosialosyl gangliosides of GM3, GM2, and GM1 (R2), and neutral GSLs of GlcCer, LacCer, Gb3, and Gb4 (R3). The nomenclature for GSLs follows the recommendations [11] of the IUB, and the ganglioside nomenclature of Svennerholm [12] was used.

Mab. The 80 kDa protein might be associated with sialylGb5 in NCR-G3 cells and thus co-immunoprecipitated by 6E2.

Comparison of reactivity to sialyl Gb5 between 6E2 and MC813-70

MC813-70 established by immunizing with human EC cell lines has been most widely used as an anti-SSEA-4 antibody (mouse IgG_3, κ) [14]. Therefore we compared the reactivities of the Mabs 6E2 and MC813-70 by flow cytometry and dot-blot immunostaining. The fluorescence intensity obtained with 6E2 was stronger than that with MC813-70 in each cell line and hRBCs (Fig. 2A). A recent flow cytometric study showed that MC813-70 strongly stains hRBCs, but other anti-sialyGb5 Mabs do not [15]. However, our data indicate that 6E2 is more reactive than MC813-70. Next we compared the reactivity of the two

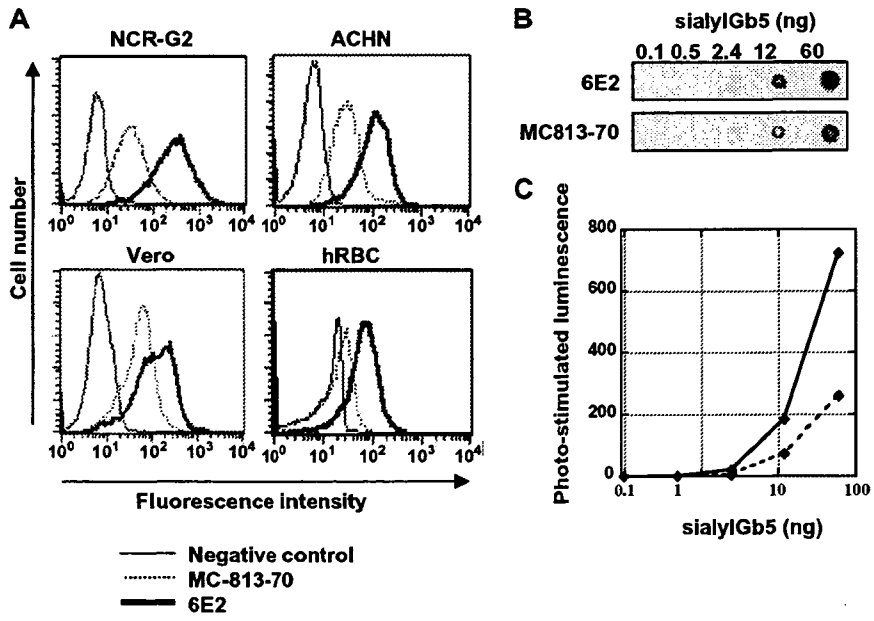

Fig. 2. Reactivity of 6E2 and MC813-70 with sialylGb5. (A) Flow cytometric analysis of SSEA-4-positive cells with 6E2. NCR-G2 cells, ACHN cells, Vero cells, and hRBCs were stained with 6E2 (bold line) or MC813-70 (dotted line) and with a FITC-conjugated secondary antibody and analyzed by flow cytometry. (B) An image of the dot-blot immunostaining of sialylGb5 obtained with a LAS-1000 luminescent imaging analyzer. (C) Measurement of antibodies bound (6E2: solid line, MC813-70: broken line).

Mabs with that of sialylGb5 by dot-blot immunostaining. Serially diluted sialylGb5 was dot-blotted onto a PVDF membrane, and the membrane was immunostained with the two Mabs. Both 6E2 and MC813-70 bound to more than 12 ng of sialylGb5, but the signals induced by 6E2 were stronger than those induced by MC813-70 (Fig. 2B,C). Thus, in addition to the flow cytometric analysis, the reactivity of 6E2 with sialylGb5 was stronger than that of MC813-70 by dot-blot immunostaining.

SSEA-4 Immunostaining of cynomolgus monkey ES cells

To confirm whether Mab 6E2 reacts with SSEA-4 on monkey ES cells, we performed an indirect immunofluorescence staining of cynomolgus monkey ES cells with Mab 6E2 and MC813-70. Mab 6E2 reacted with monkey ES cells (Fig. 3A) as well as MC-813-70 did (Fig. 3B). No difference in staining patterns of SSEA-4 between the two Mabs was observed. Mab 6E2 certainly stained SSEA-4 on monkey ES cells.

SSEA-4 immunostaining of "living" mouse preimplantation embryos without fixation

During early embryogenesis in mice, SSEA-4 had been reported to be expressed in fertilized eggs with levels gradually increasing to the morula stage and then decreasing [5]. Thus we examined the expression and distribution of SSEA-4 in preimplantation mouse embryos by immunostaining with both 6E2 and MC813-70. Both Mabs evenly stained the whole surface membranes of fixed mouse embryos, and no difference in staining pattern between the two was observed (data not shown). In order to perform a time-course of SSEA-4 distribution in a viable state, we performed immunostaining of preimplantation embryos without fixation.

3D-images of the 6E2 staining pattern obtained by confocal laser scanning microscopic observation clearly showed the localization of SSEA-4 on mouse preimplantation embryos. Two-cell embryos showed patches of SSEA-4 over the whole surface membrane with some accumulation at the interface between blastomeres (Fig. 4A). In 8-cell embryos, the amount accumulated at interfaces was further increased, as if planer membranes separate each blastomere, and some large patches were internalized but others were left on the surface membranes (Fig. 4B). The amount of SSEA-4 concentrated at the interfaces in morula was not as significant as in 8-cell embryos but still clearly observed and some patches were internalized (Fig. 4C).

2D-images of embryos stained with 6E2 showed a marked accumulation of SSEA-4 at the interfaces between blastomeres (Fig. 4D–F). These results suggest that sialylGb5 actively moves during development and tends to accumulate where blastomeres come into contact with each other.

Interestingly, however, the staining pattern of SSEA-4 using MC813-70 was different from that using 6E2. MC813-70 evenly stained the surface and the interface between blastomeres of 2-cell embryos with patches (Fig. 4G), and the amount of SSEA-4 at interfaces was not significant (Fig. 4J). In 8-cell embryos, there were patches of SSEA-4 in the central area of the outer surface of each blastomere (Fig. 4H, indicated by arrows), but the 2D-image showed that clustering also occurred at surfaces facing blastocoels (Fig. 4K, indicated by arrowheads). In morula embryos, SSEA-4 was distributed on the surface in patches and was enriched at the boundaries between blastomeres on the outer surface (Fig. 4I,L).

It remains unclear why the pattern of staining of mouse preimplantation embryos differs between 6E2 and MC813-70. The composition of fatty acids in GSLs influences the binding of antibodies [16,17] or bacterial toxins [18]. SialylGb5 recognized by the two MAbs might differ in composition of fatty acids, resulting in different immunostaining patterns. It was reported that the clustering of sialylGb5 by a Mab induces the activation of sialylGb5-associated kinases in raft microdomains of human mammary carcinoma cells, leading to downstream signaling [19,20]. The clustering of sialyGb5 by 6E2 on preimplantation mouse embryos may also induce the activation of some kinases, followed by downstream signaling. Recently, Comisky et al. suggested that lipid rafts and their associated molecules are spatiotemporally positioned to play a critical role in preimplantation developmental events [21]. The patches or clusters of sialylGb5 shown in our study suggest the presence of lipid rafts containing sialylGb5 on mouse embryos.

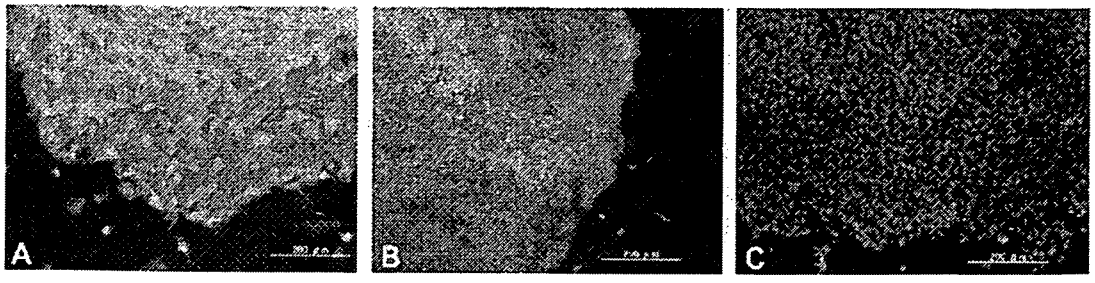

Fig. 3. Indirect immunostaining of cynomolgus monkey ES cell line CMK-6 with 6E2 and MC813-70. The CMK-6 cells were stained with 6E2 (A), MC813-70 (B), or isotype-matched mouse IgG (C), and visualized with secondary antibodies (green), followed by counterstaining of nuclei with DAPI (blue). Scale bars = 200 μm.

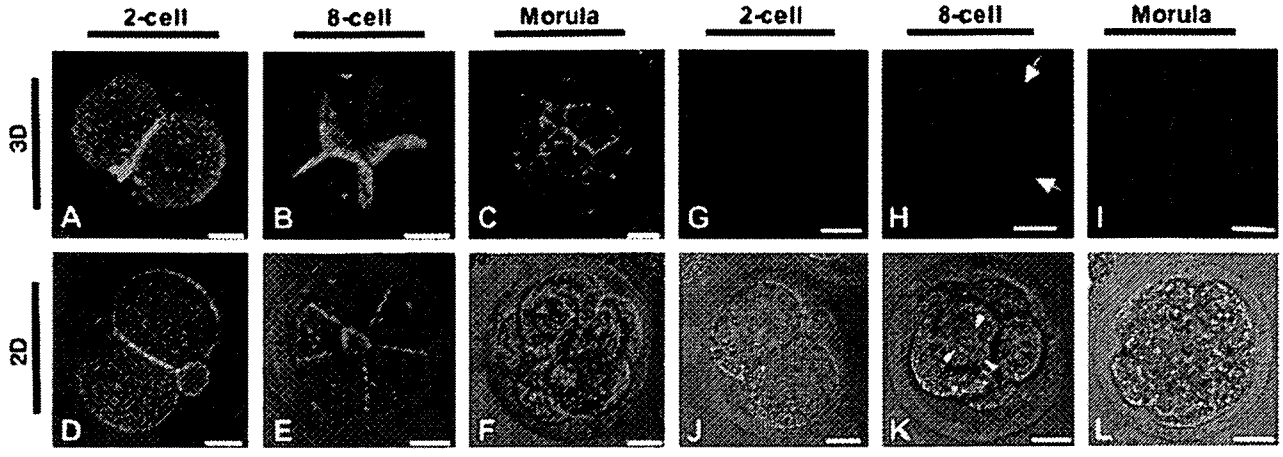

Fig. 4. Immunostaining of SSEA-4 on mouse preimplantation embryos with 6E2 and MC813-70. The embryos at the 2-cell (A, D, G, J), the 8-cell (B, E, H, K), and the morula (C, F, I, L) stages were stained with 6E2 (green) or MC813-70 (red). The panels designated 3D (A, B, C, G, H, I) are three-dimensional images reconstructed by stacking optical slice images using LSM software and the panels designated 2D (D, E, F, J, K, L) are an overlay of a fluorescent image and a differential interference contrast micrograph. Scale bars = 20 μm.

6E2 has high affinity for sialylGb5 and can be effectively conjugated with fluorescence reagents, leading to excellent staining of SSEA-4 in the surface membrane of "living" mouse preimplantation embryos. 6E2 should be of use for research into lipid rafts in early development and of great advantage for the characterization of ES cells and EC cells.

Acknowledgments

We thank S. Yamauchi for her excellent secretarial work. This work was supported in part by grants from CREST of JST and the 3rd. term comprehensive 10-year-strategy for cancer control, Research on Children and Families, Research on Human Genome Tailor made and Research on Publicly Essential Drugs and Medical Devices, Health and Labour Sciences Research Grants from the Ministry of Health, Labour and Welfare of Japan and a grant from The Japan Leukemia Research Field.

References

[1] B. Mintz, K. Illmensee, Normal genetically mosaic mice produced from malignant teratocarcinoma cells, Proc. Natl. Acad. Sci. USA 72 (1975) 3585–3589.

[2] P.W. Andrews, I. Damjanov, D. Simon, G.S. Banting, C. Carlin, N.C. Dracopoli, J. Fogh, Pluripotent embryonal carcinoma clones derived from the human teratocarcinoma cell line Tera-2. Differentiation in vivo and in vitro, Lab Invest. 50 (1984) 147–162.

[3] J.F. Jun-ichi Hata, Eizaburo Ishii, Akihiro Umezawa, Yasuo Kokai, Yoshie Matsubayashi, Hiroshi Abe, Satoru Kusakari, Haruto Kikuchi, Taketo Yamada, Tatsuya Maruyama, Differntiation of human germ cell tumor cells *in vivo* and *in vitro*, Acta Histochem. Cytochem. 25 (1992) 563–576.

[4] J.S. Draper, C. Pigott, J.A. Thomson, P.W. Andrews, Surface antigens of human embryonic stem cells: changes upon differentiation in culture, J. Anat. 200 (2002) 249–258.

[5] T. Muramatsu, H. Muramatsu, Carbohydrate antigens expressed on stem cells and early embryonic cells, Glycoconj. J. 21 (2004) 41–45.

[6] T. Nakano, A. Umezawa, H. Abe, N. Suzuki, T. Yamada, S. Nozawa, J. Hata, A monoclonal antibody that specifically reacts with human embryonal carcinomas, spermatogonia and oocytes is able to induce human EC cell death, Differentiation 58 (1995) 233–240.

[7] M. Yamamoto, N. Tase, T. Okuno, Y. Kondo, S. Akiba, N. Shimozawa, K. Terao, Monitoring of gene expression in differentiation of embryoid bodies from cynomolgus monkey embryonic stem cells in the presence of bisphenol A, J. Toxicol. Sci. 32 (2007) 301–310.

[8] Y.U. Katagiri, K. Ohmi, C. Katagiri, T. Sekino, H. Nakajima, T. Ebata, N. Kiyokawa, J. Fujimoto, Prominent immunogenicity of monosialosyl galactosylgloboside, carrying a stage-specific embryonic antigen-4 (SSEA-4) epitope in the ACHN human renal tubular cell line-a simple method for producing monoclonal antibodies against detergent-insoluble microdomains/raft, Glycoconj. J. 18 (2001) 347–353.

[9] Y.U. Katagiri, N. Kiyokawa, K. Nakamura, H. Takenouchi, T. Taguchi, H. Okita, A. Umezawa, J. Fujimoto, Laminin binding protein, 34/67 laminin receptor, carries stage-specific embryonic antigen-4 epitope defined by monoclonal antibody Raft.2, Biochem. Biophys. Res. Commun. 332 (2005) 1004–1011.

[10] K. Nakamura, Y. Hashimoto, M. Suzuki, A. Suzuki, T. Yamakawa, Characterization of GM1b in mouse spleen, J. Biochem. (Tokyo) 96 (1984) 949–957.

[11] The nomenclature of lipids (recommendations 1976). IUPAC-IUB Commission on Biochemical Nomenclature, J. Lipid. Res. 19 (1978) 114–128.

[12] L. Svennerholm, Designation and schematic structure of gangliosides and allied glycosphingolipids, Prog. Brain Res. 101 (1994) XI–XIV.

[13] L.L. Cooling, K. Kelly, Inverse expression of P(k) and Luke blood group antigens on human RBCs, Transfusion 41 (2001) 898–907.

[14] L.H. Shevinsky, B.B. Knowles, I. Damjanov, D. Solter, Monoclonal antibody to murine embryos defines a stage-specific embryonic antigen expressed on mouse embryos and human teratocarcinoma cells, Cell 30 (1982) 697–705.

[15] L. Cooling, D. Hwang, Monoclonal antibody B2, a marker of neuroendocrine sympathoadrenal precursors, recognizes the Luke (LKE) antigen, Transfusion 45 (2005) 709–716.

[16] K. Iwabuchi, I. Nagaoka, Lactosylceramide-enriched glycosphingolipid signaling domain mediates superoxide generation from human neutrophils, Blood 100 (2002) 1454–1464.

[17] K. Iwabuchi, Y. Zhang, K. Handa, D.A. Withers, P. Sinay, S. Hakomori, Reconstitution of membranes simulating "glycosignaling

domain" and their susceptibility to lyso-GM3, J. Biol. Chem. 275 (2000) 15174–15181.
[18] A. Kiarash, B. Boyd, C.A. Lingwood, Glycosphingolipid receptor function is modified by fatty acid content. Verotoxin 1 and verotoxin 2c preferentially recognize different globotriaosyl ceramide fatty acid homologues, J. Biol. Chem. 269 (1994) 11138–11146.
[19] W.F. Steelant, Y. Kawakami, A. Ito, K. Handa, E.A. Bruyneel, M. Mareel, S. Hakomori, Monosialyl-Gb5 organized with cSrc and FAK in GEM of human breast carcinoma MCF-7 cells defines their invasive properties, FEBS Lett. 531 (2002) 93–98.
[20] S. Van Slambrouck, W.F. Steelant, Clustering of monosialyl-Gb5 initiates downstream signalling events leading to invasion of MCF-7 breast cancer cells, Biochem. J. 401 (2007) 689–699.
[21] M. Comiskey, C.M. Warner, Spatio-temporal localization of membrane lipid rafts in mouse oocytes and cleaving preimplantation embryos, Dev. Biol. 303 (2007) 727–739.

0021-972X/07/$15.00/0
Printed in U.S.A.

The Journal of Clinical Endocrinology & Metabolism 92(8):3213–3218

doi: 10.1210/jc.2006-2486

Metformin Suppresses Interleukin (IL)-1β-Induced IL-8 Production, Aromatase Activation, and Proliferation of Endometriotic Stromal Cells

Yuri Takemura, Yutaka Osuga, Osamu Yoshino, Akiko Hasegawa, Tetsuya Hirata, Yasushi Hirota, Emi Nose, Chieko Morimoto, Miyuki Harada, Kaori Koga, Toshiki Tajima, Tetsu Yano, and Yuji Taketani

Department of Obstetrics and Gynecology, Faculty of Medicine, University of Tokyo, Tokyo 113-8655, Japan

Context: Metformin, a widely used treatment for diabetes that improves insulin sensitivity, also has both antiinflammatory properties and a modulatory effect on ovarian steroid production, two actions that have been suggested to be efficacious in therapy for endometriosis.

Objective: To determine whether metformin may be effective for the treatment of endometriosis, we evaluated the effects of this agent on inflammatory response, estradiol production, and proliferation of endometriotic stromal cells (ESCs).

Design: ESCs derived from ovarian endometriomas were cultured with various concentrations of metformin.

Main Outcome Measures: IL-8 production, mRNA expression and aromatase activity, and 5-bromo-2′-deoxyuridine incorporation in ESCs were measured.

Results: Metformin dose-dependently suppressed IL-1β-induced IL-8 production, cAMP-induced mRNA expression and aromatase activity, and 5-bromo-2′-deoxyuridine incorporation in ESCs.

Conclusion: These results suggest that further investigation into the unique therapeutic potential of metformin as an antiendometriotic drug is warranted. (***J Clin Endocrinol Metab* 92: 3213–3218, 2007**)

METFORMIN IS A widely used antidiabetic agent that improves insulin sensitivity (1). In reproductive medicine, the drug has been successfully used for the treatment of polycystic ovary syndrome, an etiology of which is suggested to be insulin resistance (2). Metformin may also reduce obesity-associated inflammatory status and other inflammatory responses (3–5), and has reduced serum C-reactive protein levels in women with polycystic ovary syndrome (6). In addition, it has direct effects on steroidogenesis in ovarian granulosa cells and thecal cells (7, 8).

Endometriosis is an estrogen-dependent enigmatic disease that deteriorates the health of women of reproductive age (9, 10). A large body of evidence suggests that the peritoneal inflammatory environment stimulates progress of the disease (10–14), and we and others have shown that antiinflammatory drugs have therapeutic potential for the disease (15–18). Metformin, in addition to antiinflammatory properties, has a possible modulatory effect on local steroid production, suggesting it may be active against endometriosis.

Endometriosis is characterized by inflammation, estrogen dependency, and proliferation of endometriotic cells. Here, we have evaluated the effects of metformin on markers of these pathophysiological processes in endometriotic cells as a first step toward evaluating its therapeutic application in this condition.

First Published Online May 15, 2007

Abbreviations: AMPK, AMP-activated protein kinase; BrdU, 5-bromo-2′-deoxyuridine; ESC, endometriotic stromal cell; FBS, fetal bovine serum; GAPDH, glyceraldehyde-3-phosphate dehydrogenase; LDH, lactate dehydrogenase; PPAR, peroxisome proliferator-activated receptor.

JCEM is published monthly by The Endocrine Society (http://www.endo-society.org), the foremost professional society serving the endocrine community.

Subjects and Methods

Reagents and materials

Type I collagenase and antibiotics (penicillin, streptomycin, and amphotericin B) were purchased from Sigma-Aldrich (St. Louis, MO). DMEM/Ham's F12 (F-12) medium, 0.25% trypsin-EDTA, and 0.4% trypan blue stain were from Life Technologies, Inc. (Grand Island, NY). 1, 1-Dimethylbiguanide hydrochloride (metformin), 8-bromo-cAMP, and 4-androstene-3, 17-dione (androstenedione) were obtained from Sigma-Aldrich. Recombinant IL-1β was purchased from Genzyme/Techne (Minneapolis, MN). Charcoal-stripped fetal bovine serum (FBS) was from HyClone (Logan, UT). Deoxyribonuclease I was from Invitrogen (Carlsbad, CA).

Collection of samples

Endometriotic tissues were obtained from women undergoing laparoscopy or laparotomy for ovarian endometriomas. In total, 38 women aged 24–45 yr were recruited to the present study. All women had regular menstrual cycles, and none had received hormonal treatment for at least 6 months before surgery. Symptoms of the women were pain (n = 26), infertility (n = 2), both pain and infertility (n = 6), and neither (n = 4). Menstrual phases at operation were proliferative in 18 patients and secretory in 20. Stages of endometriosis were III (n = 17) and IV (n = 21). The endometriotic tissue samples were collected from the cyst walls of ovarian endometriomas under sterile conditions for primary cell cultures.

The experimental procedures were approved by the institutional review board of the University of Tokyo, and signed informed consent for use of the sample was obtained from each woman.

Isolation and culture of human endometriotic stromal cells (ESCs)

Human ESCs were isolated and cultured as described previously (12, 19, 20). Fresh endometriotic specimens collected in sterile medium were

rinsed to remove blood cells. The tissues were minced into small pieces and incubated in DMEM/F-12, containing 25 mg/ml type I collagenase and 15 U/ml deoxyribonuclease I, for 2–3 h at 37 C, and separated using serial filtration. Debris was removed with a 100-μm nylon cell strainer (Becton Dickinson and Co., Franklin Lakes, NJ), and dispersed epithelial glands were eliminated by filtration through a 70-μm nylon cell strainer (Becton Dickinson and Co.). ESCs in the filtrate were collected by centrifugation and resuspended in phenol red-free DMEM/F-12 containing 10% charcoal-stripped FBS, 100 U/ml penicillin, 100 μg/ml streptomycin, and 250 ng/ml amphotericin B. The ESCs were seeded in a 100-mm culture plate and kept at 37 C in a humidified 5% CO_2/95% air atmosphere. At the first passage, the cells were plated into 6-, 24-, 48-, or 96-well culture plates (Becton Dickinson and Co.) at a density of 2×10^5 cells/ml in medium supplemented with 10% FBS.

The purity of the stromal cell preparations was more than 95%, as judged by positive cellular staining for vimentin and negative cellular staining for cytokeratin, CD45, CD68, and von Willebrand factor.

Measurement of IL-8

When the ESCs were approaching confluence, media were removed and replaced with fresh media and antibiotics, and the cells were cultured in serum-free media for an additional 12 h. Subsequently, the cells were incubated with or without metformin (10, 100, and 1000 μM) in serum-free media for 24 h and then stimulated with 5 ng/ml IL-1β in serum-free media for 24 h, according to our previous study (14, 20, 21). Metformin was dissolved in distilled water and then diluted 1:1000 in the medium. The doses of metformin used in the present study are similar to those used in other studies examining *in vitro* effects of metformin (4, 22). In addition, the peak plasma concentration of the drug at a standard dosage is approximately 10–20 μM (23, 24). Because local application of an antiendometriotic drug is desirable (25), we also tested metformin at relatively high concentrations. Concentrations of IL-8 in conditioned culture media were measured using a specific ELISA kit (Quantikine; R&D Systems, Minneapolis, MN) according to the manufacturer's protocol. Data were standardized by total protein of cell lysates.

RNA extraction, reverse transcription, and real-time quantitative PCR of aromatase

When the ESCs were approaching confluence, media were replaced with fresh media and antibiotics, and the cells were cultured in serum-free media for an additional 12 h. Subsequently, the cells were incubated with or without metformin (10, 100, and 1000 μM) for 24 h, and then stimulated with 1 mM cAMP for 24 h. Total RNA was extracted from the ESCs, using an RNeasy minikit (QIAGEN, Hilden, Germany). The quality of the total RNA thus obtained was confirmed by determining appropriate sharp 28S and 18S rRNA bands by agarose gel electrophoresis. One microgram of total RNA was reverse transcribed in a 20-μl volume using ReverTra Ace -α- (TOYOBO Co., Ltd., Osaka, Japan).

Aromatase mRNA expression was assessed by real-time quantitative PCR using a LightCycler according to the manufacturer's instructions (Roche Diagnostic GmbH, Mannheim, Germany). Aromatase primers (sense, 5′-CAGAGGCCAAGAGTTTGAGG-3′; antisense, 5′-ACACTAGCAGGTGGGTTTGG-3′) were chosen to amplify a 243-bp fragment. Human glyceraldehyde-3-phosphate dehydrogenase (GAPDH) primers (TOYOBO Co., Ltd.) were used to measure GAPDH mRNA levels so that expression of aromatase mRNA could be normalized to RNA loading for each sample. PCR conditions were as follows: for aromatase, 30 cycles at 95 C for 15 sec, 64 C for 8 sec, and 72 C for 10 sec; and for GAPDH, 25 cycles at 95 C for 15 sec, 64 C for 10 sec, and 72 C for 18 sec. All these PCR conditions were followed by melting curve analysis.

Each PCR product was purified with a QIAEX II gel extraction kit (QIAGEN), and their identities were confirmed using an ABI PRISM 310 genetic analyzer (Applied Biosystems, Foster City, CA).

Aromatase assay

The effect of metformin on aromatase activity was evaluated by measuring estrone levels in conditioned media of ESCs cultured with androstenedione. ESCs were seeded into 24-well plates at a density of 1×10^5 cells per well in 500 μl of the culture medium. After the ESCs were approaching confluence, the medium was replaced with fresh medium containing 2.5% FBS. The cells were incubated with or without metformin (10, 100, and 1000 μM) for 24 h and then stimulated with 1 mM cAMP for 24 h. After the treatments, 5 nM androstenedione was added to each well, and ESCs were incubated for another 24 h. The conditioned media were collected, centrifuged, and stored at −80 C for measurement of estrone levels.

Measurement of estrone

Concentrations of estrone in conditioned culture media were measured using a specific Estrone EIA kit (Yanaihara Institute Inc., Shizuoka, Japan) according to the manufacturer's protocol (26). Data were standardized by total protein of cell lysates.

5-Bromo-2′-deoxyuridine (BrdU) proliferation assay

The effect of metformin on the proliferation of ESCs was examined by measuring incorporation of BrdU into DNA. The assay was performed using a Biotrak cell proliferation ELISA system (Amersham Biosciences, Little Chalfont, UK), as previously described (12, 19, 20). Briefly, ESCs were seeded into 96-well plates at a density of 5×10^3 cells per well in 100 μl culture medium. After 24 h, the medium was replaced with fresh medium containing 2.5% FBS. After 24 or 48 h of treatment with or without metformin (10, 100, and 1000 μM), 100-μl BrdU solutions were added and incubated at 37 C for an additional 2 h. The culture medium was then removed, and the cells were fixed, and the DNA was denatured by the addition of fixative at 200 μl/well. The peroxidase-labeled anti-BrdU bound to the BrdU incorporated in newly synthesized, cellular DNA. The immune complexes were detected by the subsequent substrate reaction, and the resultant color was read at 450 nm in a DigiScan microplate reader (ASYS Hithec GmbH, Eugendorf, Austria).

Measurement of lactate dehydrogenase (LDH) release and trypan blue exclusion test

LDH release measurement and trypan blue exclusion test were conducted to examine the effect of metformin treatment on cell viability. After ESCs were treated with or without metformin (10, 100, and 1000 μM) for 24 h, conditioned media were collected, and the cells were dissociated with 0.25% trypsin-EDTA and collected by centrifugation at 200 *g* for 5 min. The release of LDH into conditioned culture media was measured using a specific Cytotoxicity Detection kit (Roche Diagnostic GmbH) according to the manufacturer's protocol. Assay medium and 2% triton X-100 solution were used for low control and high control, respectively. The ESCs were resuspended in 0.2% trypan blue solution. The number of total or trypan blue stained ESCs was counted using a microscope. Trypan blue-stained ESCs were considered dead.

Statistical analysis

Data were evaluated using ANOVA with *post hoc* analysis for multiple comparisons. P values < 0.05 were accepted as significant.

Results

Effects of metformin on IL-1β-induced IL-8 production in ESCs

IL-8 is a proinflammatory cytokine that has been implicated in the pathogenesis of the disease (11, 12, 14, 19–21, 27). We performed dose-response experiments to determine the effect of metformin on the production of IL-8 in ESCs. The concentrations of IL-8 in all samples were above the lower limit of the assay. Preincubation with metformin significantly decreased IL-1β-induced IL-8 production in ESCs in a dose-dependent manner compared with controls. The maximal effect was observed at 1000 μM, but significant decreases were seen at 10 μM (Fig. 1 and Table 1).

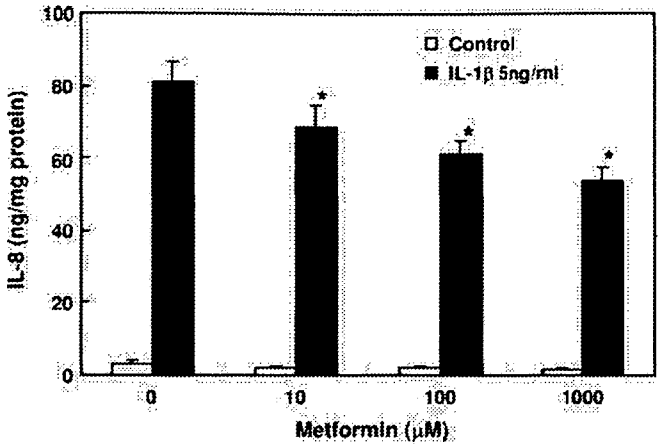

FIG. 1. Effects of metformin on IL-1β-induced IL-8 production in ESCs. ESCs were incubated with or without metformin (10, 100, and 1000 μM) for 24 h, and then stimulated with (*closed bars*) or without (*open bars*) IL-1β (5 ng/ml) for 24 h. At the end of the incubation period, conditioned media were collected and assayed for concentrations of IL-8 by ELISA. Values are the mean ± SEM of quadruplicate cultures. The results are representative of four separate experiments using samples from different women. *, $P < 0.05$ *vs.* IL-1β without metformin.

Effects of metformin on cAMP-induced mRNA expression and activity of aromatase in ESCs

Because endometriosis is estrogen dependent, we evaluated the effect of metformin on the expression of aromatase, a critical enzyme for the local production of estrogens that drive the development of the disease (28). We conducted dose-response experiments to determine the effect of metformin on cAMP-induced aromatase mRNA expression in ESCs (Fig. 2A). Metformin decreased cAMP-induced aromatase mRNA levels in ESCs in a dose-dependent manner. The maximum decrease was observed at 1000 μM, but significant decreases were seen at 100 μM.

To measure aromatase activity, ESCs were preincubated with metformin for 24 h and then stimulated with cAMP for 24 h. After incubation with 5 nM androstenedione for another 24 h, concentrations of estrone were measured. The concentrations of estrone in all conditioned culture media were above the lower limits of the assay. As depicted in Fig. 2B and Table 1, metformin decreased cAMP-induced aromatase activity in ESCs in a dose-dependent manner, with the maximal effect being observed at 1000 μM, and significant decreases seen at 10 μM.

Effects of metformin on BrdU incorporation in ESCs

Dose-response experiments were conducted to determine the effect of metformin on DNA synthesis, as a marker of cell proliferation, in ESCs. Metformin at concentrations between 10 and 1000 μM dose dependently inhibited BrdU incorporation into DNA in ESCs at 24 and 48 h of the treatment, the maximal effect being observed at 1000 μM (Fig. 3 and Table 1).

Effects of metformin on cell viability of ESCs

Metformin did not increase LDH release from ESCs, nor did it increase the number of trypan blue-stained ESCs (Table 2).

Discussion

In the present study, we have demonstrated that metformin suppressed the production of IL-1β-induced IL-8, the activation of aromatase, and the proliferation of ESCs. These effects of metformin would all be expected to limit the development of endometriosis.

IL-1β-induced secretion of IL-8 from endometriotic cells has been proposed to be a driver of endometriosis progression (29, 30). IL-8 levels are increased in the peritoneal fluid of women with endometriosis (31, 32). Interestingly, metformin has suppressed IL-8 release from human adipose tissue *in vitro* (33), and a recent report demonstrated that metformin inhibited IL-1β-induced release of IL-6 and IL-8 in human vascular wall cells (4). Although we show here that metformin can inhibit IL-1β-induced secretion of IL-8 from ESCs, at the same doses, metformin did not inhibit secretion of IL-8 from eutopic endometrial stromal cells (data not shown). Thus, metformin seems to exert its antiinflammatory role by reducing proinflammatory cytokine secretion in specific cell types.

Because endometriosis is an estrogen-dependent disease, local production of estrogen in endometriotic tissues is suggested to be important for the growth of the lesion. Numerous reports demonstrate abundant aromatase expression and elevated local estrogen production in endometriotic tissues (28), suggesting that aromatase is responsible for the local production of estrogen. Cases of endometriosis have also been successfully treated with aromatase inhibitors (34–38). A fascinating proposed mechanism is that increased prostaglandin estradiol stimulates aromatase activity via cAMP and increases estrogen production in endometriotic lesions (28). In the present study, cAMP-stimulated aromatase activity was suppressed with metformin in ESCs. Thus, metformin could be expected to suppress estrogen levels in endometriotic tissues. Interestingly, metformin has inhibited FSH and insulin-stimulated progesterone and estradiol production in granulosa cells (8). Together, metformin may inhibit endometriosis through suppression of both ovarian and local production of estrogens.

We also show that metformin inhibited BrdU uptake of ESCs. An antiproliferative effect of metformin has also been

TABLE 1. Combined data of responses of ESCs obtained from different patients

Metformin (μM)	0	10	100	1000
IL-8 (induced by IL-1 and β)	100	87.2 ± 2.8	80.6 ± 4.2	71.6 ± 2.9
Estrone (induced by cAMP)	100	86.1 ± 5.0	79.2 ± 2.3	74.8 ± 4.1
BrdU (24 h)	100	92.9 ± 1.7	88.9 ± 2.1	79.4 ± 4.4
BrdU (48 h)	100	87.0 ± 3.4	70.7 ± 5.8	58.9 ± 5.7

Mean ± SEM of the data using samples from four different individuals are shown, standardizing values without metformin as 100% in each individual.

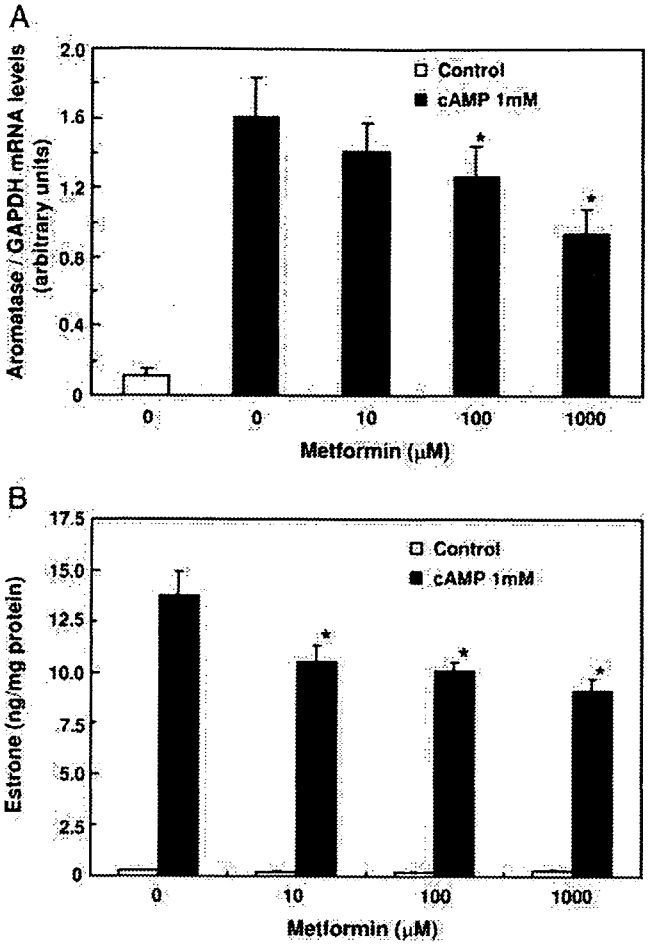

FIG. 2. Effects of metformin on mRNA expression (A) and activity (B) of aromatase induced by cAMP in ESCs. ESCs were incubated with or without metformin (10, 100, and 1000 μM) for 24 h, and then stimulated with (*closed bars*) or without (*open bars*) cAMP (1 mM) for 24 h. A, At the end of the incubation period, the total RNA isolated from the ESCs was reverse transcribed and amplified by real-time PCR using primers for aromatase. The data were calculated by subtracting the signal threshold cycles of the internal standard (GAPDH) from aromatase. Values are the mean ± SEM of six independent experiments. *, $P < 0.05$ *vs.* cAMP without metformin. B, At the end of the incubation period, androstenedione was added, and cells were incubated for a further 24 h, and conditioned media were collected and assayed for aromatase activity by Estrone EIA kit. Values represent the mean ± SEM of quadruplicate cultures. The results are representative of four separate experiments using samples from different women. *, $P < 0.03$ *vs.* cAMP without metformin.

demonstrated in leptin-stimulated vascular smooth muscle cells (39). Combined with the antiinflammatory and antiestrogenic effect of metformin, the direct antiproliferative effect on ESCs supports its therapeutic potential for endometriosis. Consistent with this, one case report described regression of atypical endometrial hyperplasia that was resistant to progestin therapy after metformin treatment (40).

What is an intracellular mechanism that underlies these diverse effects of metformin in ESCs? AMP-activated protein kinase (AMPK) is a known target of metformin action in various cells (22, 41). It is increasingly being shown to have pleiotropic actions in the regulation of the endocrine system. However, to date, the role of AMPK in endometriosis is unknown. Adiponectin is also an activator of AMPK. We have recently shown that adiponectin stimulated AMPK and inhibited inflammatory cytokine production in endometrial cells (21). In addition, we reported that serum and peritoneal fluid adiponectin levels were decreased in women with endometriosis (42, 43). Together, these suggest that AMPK may be involved in the antiinflammatory effects of metformin demonstrated in ESCs in the present study.

Recently, peroxisome proliferator-activated receptor (PPAR)-γ agonists, ciglitazone (44), and rosiglitazone (45) have regressed endometriotic lesion in a rat endometriosis model. Interestingly, like metformin, these PPAR-γ agonists are also widely used antidiabetic drugs. Similar to metformin, PPAR-γ agonists exert antiinflammatory (46) and antiproliferative effects (47), which are likely to mediate their antiendometriotic properties.

It has been argued that ovarian endometriosis is a different

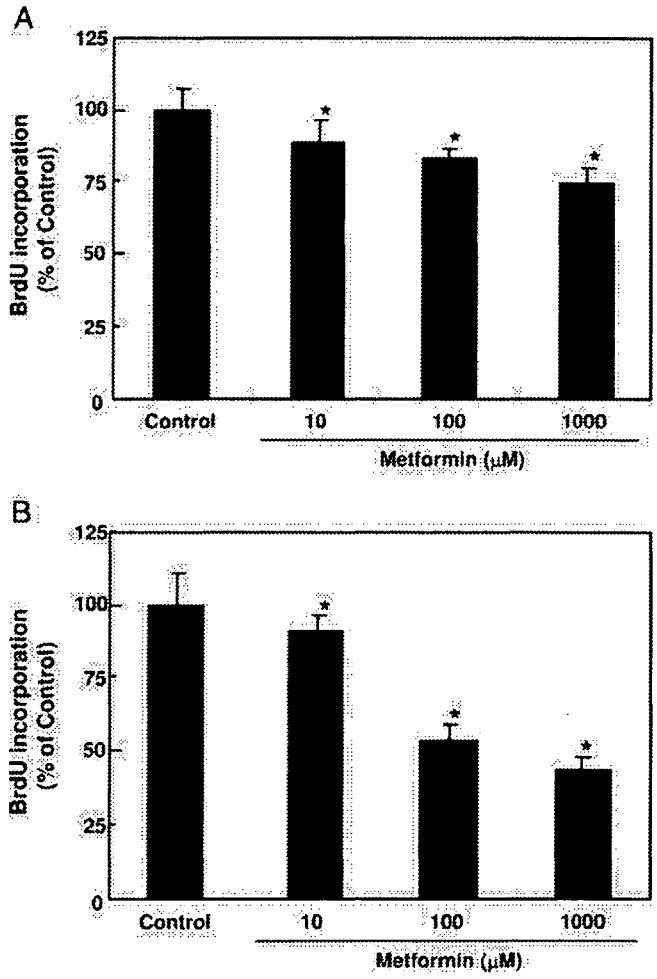

FIG. 3. Effects of metformin on BrdU incorporation in ESCs. The effect of metformin on the proliferation of ESCs was examined by measuring BrdU into DNA by using a cell proliferation ELISA system. ESCs were treated with or without metformin (10, 100, and 1000 μM) for 24 (A) or 48 h (B). Values are the mean ± SEM of sextuplicate cultures. The results are representative of four separate experiments using samples from different women. *, $P < 0.01$ *vs.* control.

TABLE 2. Effects of metformin on LDH release from ESCs and trypan blue staining of ESCs

Metformin (μM)	0	10	100	1000
LDH	8.6 ± 1.0	8.3 ± 1.0	7.8 ± 1.0	7.1 ± 0.9
Trypan blue	7.5 ± 1.3	7.5 ± 1.4	7.4 ± 1.8	7.4 ± 1.2

Mean ± SEM of the data from four (LDH) and two (trypan blue) independent experiments using ESCs from different individuals is shown. Values are shown as percentage (%) of high control (LDH) and total cells (trypan blue).

entity from peritoneal endometriosis (48), as exemplified by a recent study that showed different patterns of gene expression between ovarian and nonovarian endometriosis (49). Due to technical limitations, we only used endometriotic cells from ovarian endometrioma, and it remains possible that nonovarian endometriotic cells may show different responses to metformin from the present results.

In summary, we have shown that metformin can inhibit IL-1β-induced IL-8 production, aromatase activation, and proliferation of ESCs. These findings suggest a unique therapeutic potential for metformin as an antiendometriotic drug.

Acknowledgments

Received November 13, 2006. Accepted May 7, 2007.

Address all correspondence and requests for reprints to: Yutaka Osuga, M.D., Department of Obstetrics and Gynecology, Faculty of Medicine, University of Tokyo, 7-3-1, Hongo, Bunkyo-ku, Tokyo 113-8655, Japan. E-mail: yutakaos-tky@umin.ac.jp.

This work was partially supported by Grants-in-Aid for Scientific Research from the Ministry of Education, Culture, Sports, Science and Technology, and the Ministry of Health, Labor and Welfare.

Disclosure Information: The authors have nothing to declare.

References

1. **Goodarzi MO, Bryer-Ash M** 2005 Metformin revisited: re-evaluation of its properties and role in the pharmacopoeia of modern antidiabetic agents. Diabetes Obes Metab 7:654–665
2. **Lord J, Wilkin T** 2004 Metformin in polycystic ovary syndrome. Curr Opin Obstet Gynecol 16:481–486
3. **Bergheim I, Luyendyk JP, Steele C, Russell GK, Guo L, Roth RA, Arteel GE** 2006 Metformin prevents endotoxin-induced liver injury after partial hepatectomy. J Pharmacol Exp Ther 316:1053–1061
4. **Isoda K, Young JL, Zirlik A, MacFarlane LA, Tsuboi N, Gerdes N, Schonbeck U, Libby P** 2006 Metformin inhibits proinflammatory responses and nuclear factor-κB in human vascular wall cells. Arterioscler Thromb Vasc Biol 26:611–617
5. **Lin HZ, Yang SQ, Chuckaree C, Kuhajda F, Ronnet G, Diehl AM** 2000 Metformin reverses fatty liver disease in obese, leptin-deficient mice. Nat Med 6:998–1003
6. **Morin-Papunen L, Rautio K, Ruokonen A, Hedberg P, Puukka M, Tapanainen JS** 2003 Metformin reduces serum C-reactive protein levels in women with polycystic ovary syndrome. J Clin Endocrinol Metab 88:4649–4654
7. **Attia GR, Rainey WE, Carr BR** 2001 Metformin directly inhibits androgen production in human thecal cells. Fertil Steril 76:517–524
8. **Mansfield R, Galea R, Brincat M, Hole D, Mason H** 2003 Metformin has direct effects on human ovarian steroidogenesis. Fertil Steril 79:956–962
9. **Momoeda M, Taketani Y, Terakawa N, Hoshiai H, Tanaka K, Tsutsumi O, Osuga Y, Maruyama M, Harada T, Obata K, Hayashi K** 2002 Is endometriosis really associated with pain? Gynecol Obstet Invest 54(Suppl 1):18–21
10. **Osuga Y, Koga K, Tsutsumi O, Yano T, Maruyama M, Kugu K, Momoeda M, Taketani Y** 2002 Role of laparoscopy in the treatment of endometriosis-associated infertility. Gynecol Obstet Invest 53(Suppl 1):33–39
11. **Harada M, Osuga Y, Hirota Y, Koga K, Morimoto C, Hirata T, Yoshino O, Tsutsumi O, Yano T, Taketani Y** 2005 Mechanical stretch stimulates interleukin-8 production in endometrial stromal cells: possible implications in endometrium-related events. J Clin Endocrinol Metab 90:1144–1148
12. **Hirota Y, Osuga Y, Hirata T, Harada M, Morimoto C, Yoshino O, Koga K, Yano T, Tsutsumi O, Taketani Y** 2005 Activation of protease-activated receptor 2 stimulates proliferation and interleukin (IL)-6 and IL-8 secretion of endometriotic stromal cells. Hum Reprod 20:3547–3553
13. **Koga K, Osuga Y, Yoshino O, Hirota Y, Yano T, Tsutsumi O, Taketani Y** 2005 Elevated interleukin-16 levels in the peritoneal fluid of women with endometriosis may be a mechanism for inflammatory reactions associated with endometriosis. Fertil Steril 83:878–882
14. **Yoshino O, Osuga Y, Hirota Y, Koga K, Hirata T, Harada M, Morimoto C, Yano T, Nishii O, Tsutsumi O, Taketani Y** 2004 Possible pathophysiological roles of mitogen-activated protein kinases (MAPKs) in endometriosis. Am J Reprod Immunol 52:306–311
15. **Yoshino O, Osuga Y, Koga K, Hirota Y, Hirata T, Ruimeng X, Na L, Yano T, Tsutsumi O, Taketani Y** 2006 FR 167653, a p38 mitogen-activated protein kinase inhibitor, suppresses the development of endometriosis in a murine model. J Reprod Immunol 72:85–93
16. **D'Hooghe TM, Nugent NP, Cuneo S, Chai DC, Deer F, Debrock S, Kyama CM, Mihalyi A, Mwenda JM** 2006 Recombinant human TNFRSF1A (r-hTBP1) inhibits the development of endometriosis in baboons: a prospective, randomized, placebo- and drug-controlled study. Biol Reprod 74:131–136
17. **Dogan E, Saygili U, Posaci C, Tuna B, Caliskan S, Altunyurt S, Saatli B** 2004 Regression of endometrial explants in rats treated with the cyclooxygenase-2 inhibitor rofecoxib. Fertil Steril 82(Suppl 3):1115–1120
18. **Efstathiou JA, Sampson DA, Levine Z, Rohan RM, Zurakowski D, Folkman J, D'Amato RJ, Rupnick MA** 2005 Nonsteroidal antiinflammatory drugs differentially suppress endometriosis in a murine model. Fertil Steril 83:171–181
19. **Hirota Y, Osuga Y, Hirata T, Yoshino O, Koga K, Harada M, Morimoto C, Nose E, Yano T, Tsutsumi O, Taketani Y** 2005 Possible involvement of thrombin/protease-activated receptor 1 system in the pathogenesis of endometriosis. J Clin Endocrinol Metab 90:3673–3679
20. **Morimoto C, Osuga Y, Yano T, Takemura Y, Harada M, Hirata T, Hirota Y, Yoshino O, Koga K, Kugu K, Taketani Y** 2005 GnRH II as a possible cytostatic regulator in the development of endometriosis. Hum Reprod 20:3212–3218
21. **Takemura Y, Osuga Y, Yamauchi T, Kobayashi M, Harada M, Hirata T, Morimoto C, Hirota Y, Yoshino O, Koga K, Yano T, Kadowaki T, Taketani Y** 2006 Expression of adiponectin receptors and its possible implication in the human endometrium. Endocrinology 147:3203–3210
22. **Zhou G, Myers R, Li Y, Chen Y, Shen X, Fenyk-Melody J, Wu M, Ventre J, Doebber T, Fujii N, Musi N, Hirshman MF, Goodyear LJ, Moller DE** 2001 Role of AMP-activated protein kinase in mechanism of metformin action. J Clin Invest 108:1167–1174
23. **Pentikainen PJ, Neuvonen PJ, Penttila A** 1979 Pharmacokinetics of metformin after intravenous and oral administration to man. Eur J Clin Pharmacol 16:195–202
24. **Tucker GT, Casey C, Phillips PJ, Connor H, Ward JD, Woods HF** 1981 Metformin kinetics in healthy subjects and in patients with diabetes mellitus. Br J Clin Pharmacol 12:235–246
25. **Nomura K, Murakami K, Shozu M, Nakama T, Yui N, Inoue M** 2006 Local application of danazol-loaded hyaluronic acid hydrogel to endometriosis in a rat model. Fertil Steril 85(Suppl 1):1157–1167
26. **Ohno K, Araki N, Yanase T, Nawata H, Iida M** 2004 A novel nonradioactive method for measuring aromatase activity using a human ovarian granulosa-like tumor cell line and an estrone ELISA. Toxicol Sci 82:443–450
27. **Arici A** 2002 Local cytokines in endometrial tissue: the role of interleukin-8 in the pathogenesis of endometriosis. Ann NY Acad Sci 955:101–109
28. **Attar E, Bulun SE** 2006 Aromatase and other steroidogenic genes in endometriosis: translational aspects. Hum Reprod Update 12:49–56
29. **Akoum A, Lawson C, McColl S, Villeneuve M** 2001 Ectopic endometrial cells express high concentrations of interleukin (IL)-8 in vivo regardless of the menstrual cycle phase and respond to oestradiol by up-regulating IL-1-induced IL-8 expression in vitro. Mol Hum Reprod 7:859–866
30. **Akoum A, Lemay A, Paradis I, Rheault N, Maheux R** 1996 Secretion of interleukin-6 by human endometriotic cells and regulation by proinflammatory cytokines and sex steroids. Hum Reprod 11:2269–2275
31. **Gazvani MR, Christmas S, Quenby S, Kirwan J, Johnson PM, Kingsland CR** 1998 Peritoneal fluid concentrations of interleukin-8 in women with endometriosis: relationship to stage of disease. Hum Reprod 13:1957–1961
32. **Iwabe T, Harada T, Tsudo T, Tanikawa M, Onohara Y, Terakawa N** 1998 Pathogenetic significance of increased levels of interleukin-8 in the peritoneal fluid of patients with endometriosis. Fertil Steril 69:924–930
33. **Bruun JM, Pedersen SB, Richelsen B** 2000 Interleukin-8 production in human adipose tissue. Inhibitory effects of anti-diabetic compounds, the thiazolidinedione ciglitazone and the biguanide metformin. Horm Metab Res 32:537–541
34. **Ailawadi RK, Jobanputra S, Kataria M, Gurates B, Bulun SE** 2004 Treatment of endometriosis and chronic pelvic pain with letrozole and norethindrone acetate: a pilot study. Fertil Steril 81:290–296
35. **Razzi S, Fava A, Sartini A, De Simone S, Cobellis L, Petraglia F** 2004 Treat-

ment of severe recurrent endometriosis with an aromatase inhibitor in a young ovariectomised woman. BJOG 111:182–184
36. **Shippen ER, West Jr WJ** 2004 Successful treatment of severe endometriosis in two premenopausal women with an aromatase inhibitor. Fertil Steril 81:1395–1398
37. **Soysal S, Soysal ME, Ozer S, Gul N, Gezgin T** 2004 The effects of post-surgical administration of goserelin plus anastrozole compared to goserelin alone in patients with severe endometriosis: a prospective randomized trial. Hum Reprod 19:160–167
38. **Takayama K, Zeitoun K, Gunby RT, Sasano H, Carr BR, Bulun SE** 1998 Treatment of severe postmenopausal endometriosis with an aromatase inhibitor. Fertil Steril 69:709–713
39. **Li L, Mamputu JC, Wiemsperger N, Renier G** 2005 Signaling pathways involved in human vascular smooth muscle cell proliferation and matrix metalloproteinase-2 expression induced by leptin: inhibitory effect of metformin. Diabetes 54:2227–2234
40. **Session DR, Kalli KR, Tummon IS, Damario MA, Dumesic DA** 2003 Treatment of atypical endometrial hyperplasia with an insulin-sensitizing agent. Gynecol Endocrinol 17:405–407
41. **Kola B, Boscaro M, Rutter GA, Grossman AB, Korbonits M** 2006 Expanding role of AMPK in endocrinology. Trends Endocrinol Metab 17:205–215
42. **Takemura Y, Osuga Y, Harada M, Hirata T, Koga K, Yoshino O, Hirota Y, Morimoto C, Yano T, Taketani Y** 2005 Concentration of adiponectin in peritoneal fluid is decreased in women with endometriosis. Am J Reprod Immunol 54:217–221
43. **Takemura Y, Osuga Y, Harada M, Hirata T, Koga K, Morimoto C, Hirota Y, Yoshino O, Yano T, Taketani Y** 2005 Serum adiponectin concentrations are decreased in women with endometriosis. Hum Reprod 20:3510–3513
44. **Lebovic DI, Kir M, Casey CL** 2004 Peroxisome proliferator-activated receptor-induces regression of endometrial explants in a rat model of endometriosis. Fertil Steril 82(Suppl 3):1008–1013
45. **Demirturk F, Aytan H, Caliskan AC, Aytan P, Koseoglu DR** 2006 Effect of peroxisome proliferator-activated receptor-agonist rosiglitazone on the induction of endometriosis in an experimental rat model. J Soc Gynecol Investig 13:58–62
46. **Pritts EA, Zhao D, Ricke E, Waite L, Taylor RN** 2002 PPAR-γ decreases endometrial stromal cell transcription and translation of RANTES *in vitro*. J Clin Endocrinol Metab 87:1841–1844
47. **Houston KD, Copland JA, Broaddus RR, Gottardis MM, Fischer SM, Walker CL** 2003 Inhibition of proliferation and estrogen receptor signaling by peroxisome proliferator-activated receptor ligands in uterine leiomyoma. Cancer Res 63:1221–1227
48. **Nisolle M, Donnez J** 1997 Peritoneal endometriosis, ovarian endometriosis, and adenomyotic nodules of the rectovaginal septum are three different entities. Fertil Steril 68:585–596
49. **Wu Y, Kajdacsy-Balla A, Strawn E, Basir Z, Halverson G, Jailwala P, Wang Y, Wang X, Ghosh S, Guo SW** 2006 Transcriptional characterizations of differences between eutopic and ectopic endometrium. Endocrinology 147:232–246

JCEM is published monthly by The Endocrine Society (http://www.endo-society.org), the foremost professional society serving the endocrine community.

0013-7227/08/$15.00/0
Printed in U.S.A.

Endocrinology 149(3):1260–1267

doi: 10.1210/en.2007-0749

Interleukin (IL)-17A Stimulates IL-8 Secretion, Cyclooxygensase-2 Expression, and Cell Proliferation of Endometriotic Stromal Cells

Tetsuya Hirata, Yutaka Osuga, Kahori Hamasaki, Osamu Yoshino, Mika Ito, Akiko Hasegawa, Yuri Takemura, Yasushi Hirota, Emi Nose, Chieko Morimoto, Miyuki Harada, Kaori Koga, Toshiki Tajima, Shigeru Saito, Tetsu Yano, and Yuji Taketani

Department of Obstetrics and Gynecology (T.H., Y.O., K.H., O.Y., A.H., Y.Takem., Y.H., E.N., C.M., M.H., K.K., T.T., T.Y., Y.Taket.), Faculty of Medicine, University of Tokyo, Tokyo 113-8655, Japan; and Department of Obstetrics and Gynecology (M.I., S.S.), University of Toyama, Toyama 930-0194, Japan

IL-17A is secreted from Th17 cells, a discovery leading to revision of the mechanism underlying the role of Th1/Th2 in the immune response. Strong evidence suggests that immune responses associated with inflammation are involved in the pathogenesis of endometriosis. In the present study, we first demonstrated that the presence of Th17 cells in peritoneal fluid of endometriotic women by flow cytometric analysis and IL-17A-positive cells in endometriotic tissues by immunohistochemistry. To investigate the role of IL-17A in the development of endometriosis, we then studied the effect of IL-17A on IL-8 production, cyclooxygensase-2 expression, and cell proliferation of cultured endometriotic stromal cells (ESCs). IL-17A enhanced IL-8 secretion from ESCs in a dose-dependent manner. The IL-17A-induced secretion of IL-8 from ESCs was suppressed by anti-IL-17 receptor A antibodies or inhibitors of p38 MAPK, p42/44 MAPK, and stress-activated protein kinase/c-Jun N-terminal kinase. Addition of TNFα synergistically increased IL-17A-induced IL-8 secretion from ESCs. IL-17A also enhanced the expression of cyclooxygensase-2 mRNA and proliferation of ESCs. IL-17A may play a role in the development of endometriosis by stimulating inflammatory responses and proliferation of ESCs. (*Endocrinology* 149: 1260–1267, 2008)

ENDOMETRIOSIS, DEFINED BY the presence of viable endometriotic tissue outside the uterus, is an enigmatic disease. Implantation and growth of endometrial cells from the overflow of menstrual blood into the peritoneal cavity is a widely accepted hypothesis for the pathogenesis of endometriosis. Although retrograde menstruation is observed in most women, only a fraction develop endometriosis. Multiple lines of evidence suggest that inflammation and immune responses play a pivotal role in the pathogenesis of endometriosis (1, 2).

Recent expeditious understanding of Th17 cells substantially revised the conventional Th1/Th2 hypothesis of T cell immunology (3–5). Th17 cells, along with Th1 and Th2 cells, differentiate from naïve T cells. Interferon-γ and IL-4 are specific cytokines secreted from Th1 and Th2 cells, respectively. IL-17A is a representative cytokine secreted from Th17 cells. IL-17A, a disulfide-linked homodimeric glycoprotein consisting of 155 amino acids, has been described in various immune responses and inflammation (6).

Elevated levels of inflammatory substances and cells in the peritoneal fluid (PF) of women with endometriosis is highly indicative of pelvic cavity inflammation (7). A recent study demonstrated that increases in the level of IL-17A in PF correlate with the severity of endometriosis and infertility associated with this disorder (8).

In view of the emerging significance of IL-17A in a novel paradigm in immunology, we investigated the role of IL-17A in endometriosis. In the present study, we first examined presence of IL-17A immunoreactive cells in endometriotic tissues. In particular, we demonstrated Th17 cells in peritoneal fluid mononuclear cells (PFMCs). Thereafter, we studied effects of IL-17A on endometriotic stromal cells (ESCs). To this end, we mainly measured production of IL-8 in ESCs because IL-8 is a possible key player in endometriosis. It has been reported that IL-8 concentrations are increased in PF of endometriotic women, and IL-8 stimulates proliferation, matrix metalloproteinase activity, invasive capability, Fas ligand protein expression, and adhesion capability of endometrial stromal cells (9–11). We also examined cooperative effect of IL-17A to TNFα, another proinflammatory cytokine important for the disease (12). Finally, we studied direct proliferative effect of IL-17A on ESCs.

First Published Online December 13, 2007

Abbreviations: BrdU, 5-Bromo-2′-deoxyuridine; COX, cyclooxygenase; ESC, endometriotic stromal cell; FBS, fetal bovine serum; GAPDH, glyceraldehyde dehydrogenase; IL-17RA, antihuman IL-17 receptor; JNK, c-Jun N-terminal kinase; PF, peritoneal fluid; PFMC, PF mononuclear cell; PMA, phorbol 12-myristate 13-acetate; SAPK, stress-activated protein kinase.

Endocrinology is published monthly by The Endocrine Society (http://www.endo-society.org), the foremost professional society serving the endocrine community.

Materials and Methods

Reagents and materials

Human recombinant IL-17A, TNFα, goat antihuman IL-17A, goat IgG control, mouse antihuman IL-17 receptor (IL-17RA) and mouse IgG1 isotype control were purchased from R&D systems (Minneapolis, MN). Antibodies of human CD3, CD4, and mouse IgG1 isotype control and Goldistop were purchased from BD Bioscience (San Jose, CA). Antihuman IL-17A antibody and isotype control IgG1 were purchased from eBioscience (San Diego, CA). Antibodies of human p38 MAPK, phospho